Table II Reported number of PID

Category	Total number	Pediatric department	Internal medicine department
I. Combined T and B cell immunodeficiencies	93 (7%)	93 (8%)	0 (0%)
γc deficiency	47	47	0
Adenosine deaminase deficiency	9	9	0
Omenn syndrome	4	4	0
Others	23	23	0
Untested or undetermined	10	10	0
II. Predominantly antibody deficiencies	501 (40%)	434 (38%)	67 (71%)
BTK deficiency	182	173	9
Common variable immunodeficiency disorders	136	107	29
Selective IgG subclass deficiency	66	58	8
Selective IgA deficiency	49	34	15
Hyper IgM syndrome	34	34	0
Transient hypogammaglobulinemia of infancy	7	7	0
Others	11	7	4
Untested or undetermined	16	14	2
III. Other well-defined immunodeficiency syndromes	194 (16%)	189 (17%)	5 (5%)
Wiskott–Aldrich syndrome	60	60	0
DNA repair defects (other than those in category I)	15	15	0
DiGeorge anomaly	38	38	0
Hyper-IgE syndrome	56	52	4
Chronic mucocutaneous candidiasis	17	16	1
Others	5	5	0
Untested or undetermined	3	3	0
IV. Diseases of immune dysregulation	49 (4%)	48 (4%)	1 (1%)
Chediak–Higashi syndrome	9	8	1
Familial hemophagocytic lymphohistiocytosis syndrome	5	5	0
X-linked lymphoproliferative syndrome	8	8	0
Autoimmune lymphoproliferative syndrome	8	8	0
APECED	4	4	0
IPEX syndrome	7	7	0
Others	2	2	0
Untested or undetermined	6	6	0
V. Congenital defects of phagocyte number, function, or both	230 (19%)	223 (19%)	7 (8%)
Severe congenital neutropenia	44	42	2
Cyclic neutropenia	19	17	2
Chronic granulomatous disease	147	144	3
Mendelian susceptibility to mycobacterial disease	5	5	0
Others	9	9	0
Untested or undetermined	6	6	0
VI. Defects in innate immunity	15 (1%)	15 (1%)	0
Anhidrotic ectodermal dysplasia with immunodeficiency	7	7	0
Interleukin-1 receptor-associated kinase 4 deficiency	2	2	0
Others	5	5	0
Untested or undetermined	1	1	0
VII. Autoinflammatory disorders	108 (9%)	101 (9%)	7 (8%)
Familial Mediterranean fever	44	40	4
TNF receptor-associated periodic syndrome	13	12	1
Hyper IgD syndrome	4	4	0
Cryopyrin-associated periodic syndrome	22	22	0

Table II (continued)

Category	Total number	Pediatric department	Internal medicine department
Others	3	3	0
Untested or undetermined	22	20	2
VIII. Complement deficiencies	32 (3%)	29 (3%)	3 (3%)
IX. Undetermined	18 (1%)	14 (1%)	4 (4%)
Total	1,240	1,146	94

APECED Autoimmune polyendocrinopathy with candidiasis and ectodermal dystrophy, *IPEX* immune dysregulation, polyendocrinopathy, enteropathy, X-linked

increasing age (Fig. 2b). The median age of CID, BTK deficiency, CVID, and CGD patients was 5.2, 12.8, 25.1, and 14.7 years, respectively.

It is well known that PID patients are susceptible to many pathogens and experience community-acquired or opportunistic infections. In this study, we focused on noninfectious complications of PID because they have been less well studied on a large scale and may provide important information for improving the quality of life of PID patients. Twenty-five PID patients developed malignant disorders (2.7%; Table III). Lymphoma, in particular, Epstein–Barr virus-related, and leukemia were dominant, while there were no patients with gastric carcinoma. CVID, Wiskott–Aldrich syndrome (WAS), and ataxia telangiectasia were more frequently associated with malignant diseases among PID patients. A case of Mendelian susceptibility

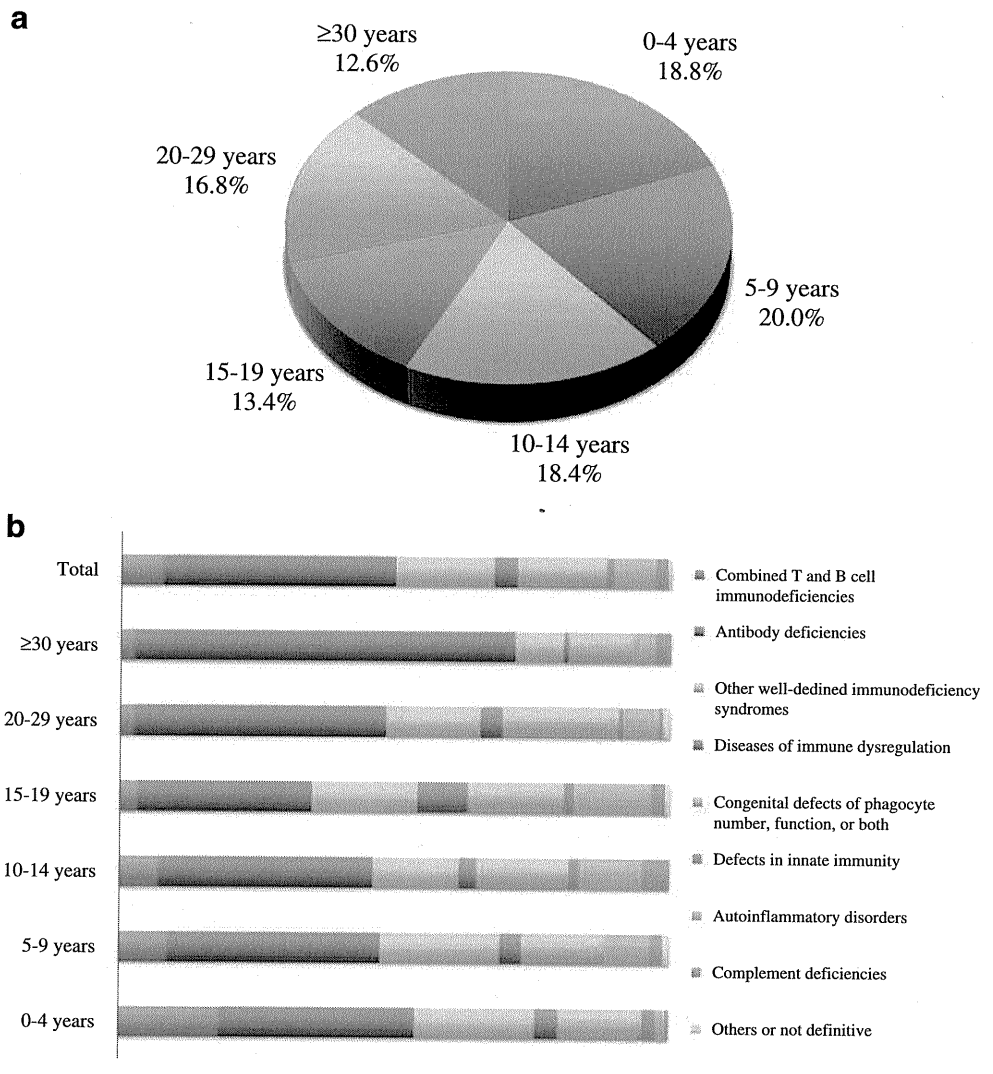

Fig. 2 **a** Age distribution of PID patients. **b** Distribution of PID in each age group

to mycobacterial disease with squamous cell carcinoma was also observed [9] (Table III).

Seventy-eight PID patients had immune-related (autoimmune) diseases (8.5%; Table IVa). Autoimmune lymphoproliferative syndrome, immune dysregulation, polyendocrinopathy, enteropathy X-linked (IPEX) syndrome, and nuclear factor kappa B essential modulator (NEMO) deficiency were associated with immune-related diseases at a very high incidence. In addition, immune-related diseases were relatively common in CGD and CVID patients (Table IVa). The most commonly observed immune-related disease was inflammatory bowel disease (33 cases), which was most frequently observed in CGD patients, followed by immune thrombocytopenic purpura (13 cases), autoimmune hemolytic anemia (8 cases), and systemic lupus erythematosus (SLE; 8 cases; Table IVa and b). Kawasaki disease occurred in WAS and CGD patients. In addition, this is the first report of Kawasaki disease in patients with complement deficiency (C9) and familial Mediterranean fever (FMF). A patient with warts, hypogammaglobulinemia, infections, and myelokathexis (WHIM) syndrome and a patient with tumor necrosis factor receptor-associated periodic syndrome (TRAPS) were first reported as cases of type 1 diabetes mellitus and SLE, respectively [10, 11].

Discussion

We conducted a nationwide survey of PID for the first time in 30 years and report the prevalence of PID in Japan. We registered 1,240 PID patients and found that the estimated prevalence of PID (2.3/100,000) is higher than that previously reported (1.0/100,000) in Japan. Our results are equivalent to those reported in Singapore (2.7/100,000) and Taiwan (0.77–2.17/100,000) [12–14]. However, our values are lower than those reported in Middle Eastern countries such as Kuwait (11.98/100,000) or in European countries such as France (4.4/100,000) [5–7, 15]. The high rate of consanguinity may be a cause of the high prevalence rate of PID reported in Middle Eastern countries [6, 15]. There may has been sample selection bias in this study because some asymptomatic cases (SIgAD, etc.), clinically recovered cases (transient hypogammaglobulinemia of infancy, etc.), and cases in which patients were deceased were not registered. In addition, lack of recognition of PID in internal medicine departments, not just the low response rate, might also have influenced the estimated prevalence of PID as well as the age and disease distribution. The regional prevalence of PIDs in Japan was homogenous, unlike in other countries in which a higher prevalence was

Table III Malignancies in PID patients

Primary immunodeficiency	Total	*n*	Malignancy
I. Combined T and B cell immunodeficiencies	75	2	(2.7%)
Ommen syndrome	3	1	NHL (EBV+) 1[a]
Adenosine deaminase deficiency	4	1	Breast carcinoma 1
II. Predominantly antibody deficiencies	378	8	(2.1%)
Common variable immunodeficiency disorders	93	7	HL 2, ML 2, ALL 1, Basal cell carcinoma 1, Cervical carcinoma 1
Good syndrome	4	1	Double primary carcinoma of breast and colon 1
III. Other well-defined immunodeficiency syndromes	165	7	(4.2%)
Wiskott–Aldrich syndrome	57	5	NHL 3, NHL/HL 1, LPD (EBV-) 1
Ataxia telangiectasia	13	2	T-ALL 1, MDS 1
IV. Diseases of immune dysregulation	38	4	(10.5%)
X-linked lymphoproliferative syndrome	5	2	Burkitt lymphoma 2
Autoimmune lymphoproliferative syndrome	6	2	HL (EBV+) 1, Brain tumor 1
V. Congenital defects of phagocyte number, function, or both	153	4	(2.6%)
Severe congenital neutropenia	35	3	MDS 3 (including 2 cases with monosomy 7)
MSMD	7	1	Squamous cell carcinoma of finger 1
VI. Defects in innate immunity	12	0	(0%)
VII. Autoinflammatory disorders	74	0	(0%)
VIII. Complement deficiencies	23	0	(0%)
IX. Undetermined	5	0	(0%)
Total	923	25	(2.7%)

n Number of PID patients who had malignant disorders, *ALL* acute lymphoblastic leukemia, *EBV* Epstein-Barr virus, *HL* Hodgkin lymphoma, *LPD* lymphoproliferative disease, *MDS* myelodysplastic syndrome, *ML* malignant lymphoma, *MSMD* Mendelian susceptibility to mycobacterial disease, *NHL* non-Hodgkin lymphoma

[a] The number of patients

Table IV Immune-related diseases in PID patients

(a) Immune-related diseases with each PID

Primary immunodeficiency	Total	*n*	Immune-related disease
I. Combined T and B cell immunodeficiencies	75	2	(2.6%)
MHC class II deficiency (suspected)	1	1	ITP with AIHA 1[a]
CD4 deficiency	1	1	Hashimoto disease 1
II. Predominantly antibody deficiencies	378	24	(6.3%)
Common variable immunodeficiency disorders	93	16	ITP 3, RA 2, AIHA 2, Hashimoto's disease 2, IBD 2, SLE 1, MG 1, ADEM 1, Autoimmune hepatitis 1, Uveitis 1
Hyper-IgM syndrome	32	3	JIA 1, SLE (complicated with C1q deficiency) 1, IBD 1
Selective IgA deficiency	28	3	SLE 1, SLE with Kikuchi disease 1, RA 1
IgG subclass deficiency	50	2	ITP with AIHA 1, ITP with MS 1
III. Other well-defined immunodeficiency syndromes	165	5	(3.0%)
Wiskott–Aldrich syndrome	57	3	AIHA 2, Kawasaki disease 1
DiGeorge syndrome	33	2	AIHA 1, ITP 1
IV. Diseases of immune dysregulation	38	10	(26.3%)
X-linked lymphoproliferative syndrome	5	1	IBD 1
Autoimmune lymphoproliferative syndrome	6	4	ITP 3, Graves' disease with IBD 1
APECED	5	1	T1DM with Hashimoto's disease and Vogt–Koyanagi–Harada disease 1
IPEX syndrome	6	4	T1DM 1, T1DM with ITP, AIN and IBD 1, Autoimmune enteritis 1, AIHA with Autoimmune enteritis and Hashimoto's disease 1
V. Congenital defects of phagocyte number, function, or both	153	25	(16.3%)
Chronic granulomatous disease	87	25	IBD 20, ITP 2, JIA 1, MCTD 1, Kawasaki disease 1
VI. Defects in innate immunity	12	5	(41.7%)
NEMO deficiency	7	4	IBD 3, IBD with JIA 1
WHIM syndrome	3	1	T1DM 1
VII. Autoinflammatory disorders	74	3	(4.0%)
Familial Mediterranean fever	36	2	SLE 1, Kawasaki disease 1
TNF receptor associated periodic syndrome	9	1	SLE 1
VIII. Complement deficiencies	23	3	(13.0%)
C4 deficiency	1	1	SLE with RA 1
C6 deficiency	1	1	IBD 1
C9 deficiency	11	1	Kawasaki disease 1
IX. Undetermined	5	1	(20%)
Nakajo syndrome	1	1	SLE 1
Total	923	78	(8.5 %)

(b) Immune-related manifestations associated with PID

Immune-related diseases	*n*
IBD (including autoimmune enteritis)	33
ITP	13
AIHA	8
SLE	8
RA/JIA	6
Hashimoto's disease/Graves' disease	5
Kawasaki disease	4
T1DM	4
Uveitis (including Vogt–Koyanagi–Harada disease)	2
ADEM/MS	2
Others	5

n Number of PID patients who had immune-related disorders, *ADEM* acute disseminated encephalomyelitis, *AIHA* autoimmune hemolytic anemia, *AIN* autoimmune neutropenia, *APECED* autoimmune polyendocrinopathy candidiasis ectodermal dystrophy, *IBD* inflammatory bowel disease, *IPEX* immunodysregulation, polyendocrinopathy, enteropathy X-linked, *ITP* immune thrombocytopenic purpura, *JIA* juvenile idiopathic arthritis, *MCTD* mixed connective tissue disease, *MG* myasthenia gravis, *MS* multiple sclerosis, *RA* rheumatoid arthritis, *SLE* systemic lupus erythematosus, *T1DM* type 1 diabetes mellitus, *WHIM* warts, hypogammaglobulinemia, infections, and myelokathexis

[a] The number of patients

observed in urban areas [5, 7, 16]. This may be because many PID patients were treated or followed by PID specialists distributed nationwide in Japan; this is assumed by the location of hospitals with which they were affiliated.

The distribution ratios of BTK deficiency (14.7%) and CGD (11.9%) in Japan were higher than those in a previous report from Europe (5.87% and 4.33%, respectively), while those of CIDs and other well-defined immunodeficiency syndromes were comparable [17]. The prevalence of BTK deficiency was previously reported to be 1/900,000–1,400,000 in a European cohort study [18]. In contrast, this value was estimated to be 1/300,000 in Japan in our study. BTK deficiency appears to be common in Japan, although this may be partially because more patients, including those showing atypical clinical manifestations, were diagnosed more accurately by the recently established genetic diagnostic network in Japan [19]. This is supported by the highest proportion of Japanese patients in the international mutation database for X-linked agammaglobulinemia (BTKbase) [20]. The reason for the low number of registered CGD patients in Europe in a recent report (1/620,000) [17] is unknown; the prevalence of CGD was 1 in 250,000 in a previous European survey [21], which was similar to our results (1 in 380,000 in this study and 1 in 280,000 in our previous study [22]). The percentage of BTK deficiency and CGD would be lower if more adult cases were registered because the prevalence of these disorders is low in adults. CVID was the most commonly reported PID (20.7%) in Europe, and the onset of symptoms was observed most commonly in the third decade of life in these patients [17, 23]. In this study, CVID constituted 11.0% (136 cases) of PID cases, and only 29 cases were reported from internal medicine departments (Table II). A lower number of registered CVID patients may have led to a lower number of reported patients with antibody deficiency and a lower prevalence of PID, although it is still possible that CVID is not as common in Japan as in European countries. There was no significant difference in the distribution rate of SIgAD between Japanese and Europeans, although SIgAD is rare in Japanese (1/18,500) compared with Caucasians (1/330–2,200) according to seroepidemiologic studies [24]. This may be because most SIgAD patients lack clinical manifestations. The distribution ratio of autoinflammatory disorders in Japan (9%) was much higher than that in Europe (1.02%) [17] (Table II). Considering the disease type of the autoinflammatory disorders was not specified in 22 cases (20%), it is possible that many other patients with autoinflammatory disorders remain undiagnosed in Japan as well as in other countries.

The percentage of men (69.7%) with PID is higher in Japan than in Europe (60.8%) or Kuwait (61.8%), but is equivalent to that in Taiwan (70.2%) [6, 13, 17]. The higher ratio of men, particularly in younger generation (<15 years), appears to be due to the larger number of X-linked PID patients (BTK deficiency, X-CGD, γc deficiency, etc.) in this study compared to that in Europe or Kuwait. Adolescents or adults (≥15 years) constituted 42.8% of the patients in this study, which is equivalent to the number in the European study (≥16 years: 46.6%), while those >16 years constituted only 10.9% in the previous survey [3, 17]. In this study, it was found that CVID and SIgAD are common in adults (Table II) and that antibody deficiencies are more common with increasing age (Fig. 2b). A reason for the increased number of adult PID patients may be long-term survival of PID patients due to improved treatments such as immunoglobulin replacement therapy. In addition, an increased likelihood of patients being diagnosed by internists as having late-onset PID, e.g., CVID and SIgAD, may have contributed to these values [17, 25, 26]. Therefore, it is important for internists to be well-informed regarding PID. In contrast, CIDs are fatal during infancy without hematopoietic stem cell transplantation or gene therapy. Because hematopoietic stem cell transplantation has been widely performed in Japan since the 1990s, surviving patients with CID are limited to the younger generation, similar to French patients (Fig. 2b) [5, 27, 28].

It has been reported that PID patients are at increased risk of developing malignant diseases, in particular, non-Hodgkin lymphoma, leukemia, and stomach cancer [29]. Although lymphoma and leukemia were relatively common, stomach cancer was not observed in our study. In the previous survey in Japan, eight of nine PID patients with malignant disorders (including one gastric cancer patient) died [3]. It is possible that some PID patients with malignant disorders were not registered because they were deceased. PID is also associated with immune-related diseases because of a defect in the mechanisms to control self-reactive B and T cells. The frequency of immune-related manifestations varied among individual PID patients, as reported previously [30, 31]. Four PID patients who had developed Kawasaki disease, one patient with WHIM syndrome and type 1 diabetes mellitus, and one patient with TRAPS and SLE in our study may provide new pathophysiological insights of these diseases and the association between PID and autoimmune diseases.

Conclusions

We report the prevalence and clinical characteristics of PIDs in Japan. Although the advances in diagnostic technologies and treatments have improved the prognoses of PID, many patients continue to experience severe complications such as malignancy and immune-related diseases as well as infections. To improve the quality of life of PID patients, it is necessary to pay attention to

complications and treat them appropriately. Web-based PID databases and consultation systems have been created in Japan (Primary Immunodeficiency Database in Japan [4] and Resource of Asian Primary Immunodeficiency Diseases in Asian countries [32]) to reveal precise information regarding PID and to promote cooperation between doctors and researchers [19].

Acknowledgments The authors would like to thank the support of the Japanese Research Group on Primary Immunodeficiency Diseases, which is supported by Japan's Ministry of Health, Labour and Welfare.

Conflict of Interest There is no actual or potential conflict of interest in relation to the study.

References

1. Notarangelo LD. Primary immunodeficiencies. J Allergy Clin Immunol. 2010;125(2 Suppl 2):S182–94.
2. Geha RS, Notarangelo LD, Casanova JL, Chapel H, Conley ME, Fischer A, et al. Primary immunodeficiency diseases: an update from the international union of immunological societies primary immunodeficiency diseases classification committee. J Allergy Clin Immunol. 2007;120(4):776–94.
3. Hayakawa H, Iwata T, Yata J, Kobayashi N. Primary immunodeficiency syndrome in Japan. I. overview of a nationwide survey on primary immunodeficiency syndrome. J Clin Immunol. 1981;1 (1):31–9.
4. Primary Immunodeficiency Database in Japan (PIDJ). http://pidj.rcai.riken.jp/ (in Japanese).
5. CEREDIH. The French PID study group. The French national registry of primary immunodeficiency diseases. Clin Immunol. 2010;135(2):264–72.
6. Al-Herz W. Primary immunodeficiency disorders in Kuwait: first report from Kuwait national primary immunodeficiency registry (2004–2006). J Clin Immunol. 2008;28(2):186–93.
7. Stray-Pedersen A, Abrahamsen TG, Froland SS. Primary immunodeficiency diseases in Norway. J Clin Immunol. 2000;20(6):477–85.
8. Nakamura Y, Matsumoto T, Tamakoshi A, Kawamura T, Seino Y, Kasuga M, et al. Prevalence of idiopathic hypoparathyroidism and pseudohypoparathyroidism in Japan. J Epidemiol. 2000;10(1):29–33.
9. Toyoda H, Ido M, Nakanishi K, Nakano T, Kamiya H, Matsumine A, et al. Multiple cutaneous squamous cell carcinomas in a patient with interferon gamma receptor 2 (IFN gamma R2) deficiency. J Med Genet. 2010;47(9):631–4.
10. Takaya J, Fujii Y, Higashino H, Taniuchi S, Nakamura M, Kaneko K. A case of WHIM syndrome associated with diabetes and hypothyroidism. Pediatr Diabetes. 2009;10(7):484–6.
11. Ida H, Kawasaki E, Miyashita T, Tanaka F, Kamachi M, Izumi Y, et al. A novel mutation (T61I) in the gene encoding tumour necrosis factor receptor superfamily 1A (TNFRSF1A) in a Japanese patient with tumour necrosis factor receptor-associated periodic syndrome (TRAPS) associated with systemic lupus erythematosus. Rheumatology (Oxford). 2004;43(10):1292–9.
12. Lim DL, Thong BY, Ho SY, Shek LP, Lou J, Leong KP, et al. Primary immunodeficiency diseases in Singapore—the last 11 years. Singapore Med J. 2003;44(11):579–86.
13. Lee WI, Kuo ML, Huang JL, Lin SJ, Wu CJ. Distribution and clinical aspects of primary immunodeficiencies in a Taiwan pediatric tertiary hospital during a 20-year period. J Clin Immunol. 2005;25(2):162–73.
14. Lee WI, Huang JL, Jaing TH, Shyur SD, Yang KD, Chien YH, et al. Distribution, clinical features and treatment in Taiwanese patients with symptomatic primary immunodeficiency diseases (PIDs) in a nationwide population-based study during 1985–2010. Immunobiology. 2011 Jun 21 [Epub ahead of print].
15. Shabestari MS, Maljaei SH, Baradaran R, Barzegar M, Hashemi F, Mesri A, et al. Distribution of primary immunodeficiency diseases in the Turk ethnic group, living in the northwestern Iran. J Clin Immunol. 2007;27(5):510–6.
16. Matamoros Flori N, Mila Llambi J, Espanol Boren T, Raga Borja S, Fontan Casariego G. Primary immunodeficiency syndrome in Spain: first report of the national registry in children and adults. J Clin Immunol. 1997;17(4):333–9.
17. Gathmann B, Grimbacher B, Beaute J, Dudoit Y, Mahlaoui N, Fischer A, et al. The European internet-based patient and research database for primary immunodeficiencies: results 2006–2008. Clin Exp Immunol. 2009;157 Suppl 1:3–11.
18. Toth B, Volokha A, Mihas A, Pac M, Bernatowska E, Kondratenko I, et al. Genetic and demographic features of X-linked agammaglobulinemia in Eastern and Central Europe: a cohort study. Mol Immunol. 2009;46(10):2140–6.
19. Burrows PD, Fischer A. Building networks for immunodeficiency diseases and immunology training. Nat Immunol. 2008;9(9):1005–7.
20. Valiaho J, Smith CI, Vihinen M. BTKbase: the mutation database for X-linked agammaglobulinemia. Hum Mutat. 2006;27 (12):1209–17.
21. van den Berg JM, van Koppen E, Ahlin A, Belohradsky BH, Bernatowska E, Corbeel L, et al. Chronic granulomatous disease: the European experience. PLoS One. 2009;4(4):e5234.
22. Hasui M. Chronic granulomatous disease in Japan: incidence and natural history. The study group of phagocyte disorders of Japan. Pediatr Int. 1999;41(5):589–93.
23. Chapel H, Lucas M, Lee M, Bjorkander J, Webster D, Grimbacher B, et al. Common variable immunodeficiency disorders: division into distinct clinical phenotypes. Blood. 2008;112(2):277–86.
24. Kanoh T, Mizumoto T, Yasuda N, Koya M, Ohno Y, Uchino H, et al. Selective IgA deficiency in Japanese blood donors: frequency and statistical analysis. Vox Sang. 1986;50(2):81–6.
25. Aghamohammadi A, Moin M, Farhoudi A, Rezaei N, Pourpak Z, Movahedi M, et al. Efficacy of intravenous immunoglobulin on the prevention of pneumonia in patients with agammaglobulinemia. FEMS Immunol Med Microbiol. 2004;40(2):113–8.
26. Quartier P, Debre M, De Blic J, de Sauverzac R, Sayegh N, Jabado N, et al. Early and prolonged intravenous immunoglobulin replacement therapy in childhood agammaglobulinemia: a retrospective survey of 31 patients. J Pediatr. 1999;134(5):589–96.
27. Sakata N, Kawa K, Kato K, Yabe H, Yabe M, Nagasawa M, et al. Unrelated donor marrow transplantation for congenital immunodeficiency and metabolic disease: an update of the experience of the Japan marrow donor program. Int J Hematol. 2004;80(2):174–82.
28. Morio T, Atsuta Y, Tomizawa D, Nagamura-Inoue T, Kato K, Ariga T, et al. Outcome of unrelated umbilical cord blood transplantation in 88 patients with primary immunodeficiency in Japan. Br J Haematol. 2011;154(3):363–72.
29. Vajdic CM, Mao L, van Leeuwen MT, Kirkpatrick P, Grulich AE, Riminton S. Are antibody deficiency disorders associated with a narrower range of cancers than other forms of immunodeficiency? Blood. 2010;116(8):1228–34.
30. Bussone G, Mouthon L. Autoimmune manifestations in primary immune deficiencies. Autoimmun Rev. 2009;8(4):332–6.
31. Arason GJ, Jorgensen GH, Ludviksson BR. Primary immunodeficiency and autoimmunity: lessons from human diseases. Scand J Immunol. 2010;71(5):317–28.
32. Resource of Asian primary immunodeficiency diseases (RAPID). http://rapid.rcai.riken.jp/RAPID/.

In conclusion, the associations among asthma, biofilm-forming bacteria, and revision ESS are strong and robust after adjusting for other factors in patients with CRS from a tertiary medical center. Despite its limitations, this study may improve our understanding of refractory CRS pathogenesis, possibly leading to more effective treatment strategies, such as incorporating the treatments of asthma and biofilm infection into conventional CRS therapies. Prospective cohort studies in diverse populations are needed to assess the causality of these associations.

We thank Alexander Chiu for providing the clinical samples, Andrew Cucchiara for helping with the data cleansing and analysis, and Jennifer Kofonow, Anthony Prince, Jacob Steiger, Michael Cohen, Edwin Tamashiro, and Natalia Goldstein for performing the Calgary biofilm assay and organizing the data.

Zi Zhang, MD[a]
Darren R. Linkin, MD, MSCE[b]
Brian S. Finkelman, BS[a]
Bert W. O'Malley, Jr, MD[c]
Erica R. Thaler, MD[c]
Laurel Doghramji, RN, BSN[c]
David W. Kennedy, MD[c]
Noam A. Cohen, MD, PhD[c]
James N. Palmer, MD[c]

From [a]the Center for Clinical Epidemiology and Biostatistics, [b]the Department of Medicine, Division of Infectious Diseases, and [c]the Department of Otorhinolaryngology–Head and Neck Surgery, University of Pennsylvania School of Medicine, Philadelphia, Pa. E-mail: james.palmer@uphs.upenn.edu.

Supported by the Flight Attendant Medical Research Institute Clinical Investigator Award (053367 to N.A.C. and 052414 to J.N.P.).

Disclosure of potential conflict of interest: J. N. Palmer receives research support from the Flight Attendant Medical Research Institute, has provided legal consultation/expert witness testimony in cases related to complications in sinus surgery, and is a member of the board of directors for the American Rhinologic Society. D. W. Kennedy is the medical director of ENT Care and a member of RhinActive. N. A. Cohen receives research support from the Flight Attendant Medical Research Institute. The rest of the authors have declared that they have no conflict of interest.

REFERENCES

1. Fokkens W, Lund V, Mullol J. EP3OS 2007: European position paper on rhinosinusitis and nasal polyps 2007: a summary for otorhinolaryngologists. Rhinology 2007; 45:97-101.
2. Newman LJ, Platts-Mills TA, Phillips CD, Hazen KC, Gross CW. Chronic sinusitis: relationship of computed tomographic findings to allergy, asthma, and eosinophilia. JAMA 1994;271:363-7.
3. Psaltis AJ, Weitzel EK, Ha KR, Wormald PJ. The effect of bacterial biofilms on post-sinus surgical outcomes. Am J Rhinol 2008;22:1-6.
4. Prince AA, Steiger JD, Khalid AN, Dogrhamji L, Reger C, Eau Claire S, et al. Prevalence of biofilm-forming bacteria in chronic rhinosinusitis. Am J Rhinol 2008;22: 239-45.
5. Meltzer EO, Hamilos DL, Hadley JA, Lanza DC, Marple BF, Nicklas RA, et al. Rhinosinusitis: establishing definitions for clinical research and patient care. J Allergy Clin Immunol 2004;114:155-212.
6. National Asthma Education and Prevention Program. Expert Panel Report 3 (EPR-3): guidelines for the diagnosis and management of asthma-summary report 2007. J Allergy Clin Immunol 2007;120:S94-S138.
7. Banerji A, Piccirillo JF, Thawley SE, Levitt RG, Schechtman KB, Kramper MA, et al. Chronic rhinosinusitis patients with polyps or polypoid mucosa have a greater burden of illness. Am J Rhinol 2007;21:19-26.
8. Costerton JW, Stewart PS, Greenberg EP. Bacterial biofilms: a common cause of persistent infections. Science 1999;284:1318-22.
9. Richtsmeier WJ. Top 10 reasons for endoscopic maxillary sinus surgery failure. Laryngoscope 2001;111:1952-6.

Available online March 24, 2011.
doi:10.1016/j.jaci.2011.02.022

Quantification of κ-deleting recombination excision circles in Guthrie cards for the identification of early B-cell maturation defects

To the Editor:

X-linked agammaglobulinemia (XLA) is a primary immunodeficiency caused by severely decreased numbers of mature peripheral B lymphocytes as a result of a mutation in the *BTK* gene. Non-XLA is characterized by hypogammaglobulinemia with decreased B-cell counts (less than 2% of mature B cells) in the absence of the *BTK* gene mutation. Both XLA and non-XLA are caused by an early B-cell maturation defect.[1] In patients with XLA and non-XLA, recurrent infections appear between 3 and 18 months of age, whereas the mean age at diagnosis is 3 years.[2] This delayed diagnosis results in frequent hospitalization because of pneumonia, sepsis, meningitis, and other bacterial infections, which frequently require intravenous administration of antibiotics and can be fatal. Frequent pneumonia results in a high incidence of chronic lung diseases.[3] Thus, early diagnosis and early treatment, including periodical intravenous immunoglobulin replacement therapy, is essential to improve the prognosis and the quality of life of patients with XLA and non-XLA.

In the process of B-cell maturation, immunoglobulin κ-deleting recombination excision circles (KRECs) are produced during κ-deleting recombination allelic exclusion and isotypic exclusion of the λ chain.[4] Coding joint (cj) KRECs reside within the chromosome, whereas signal joint (sj) KRECs are excised from genomic DNA. cjKREC levels remain the same after B-cell division, whereas sjKREC levels decrease, because sjKRECs are not replicated during cell division.[5] Because the B-cell maturation defects in XLA and non-XLA occur before κ-deleting recombination, KRECs are not supposed to be produced. Therefore, measurements of KRECs have the potential to be applied to the identification of these types of B-cell deficiencies in patients, which consist of around 20% of all B-cell defects.[6] In addition, some types of combined immunodeficiencies show an arrest in B-cell maturation and can also be identified by this method. The success of newborn screening for T-cell deficiencies by measuring T-cell–receptor excision circles[7] prompted us to develop a newborn screening method for XLA and non-XLA by measuring KRECs derived from neonatal Guthrie cards.

The study protocol was approved by the National Defense Medical College institutional review board, and written informed consent was obtained from the parents of normal controls, the affected children, and adult patients, in accordance with the Declaration of Helsinki.

First, we determined the sensitivity of detection levels of cjKRECs and sjKRECs in Guthrie cards using real-time quantitative PCR.[5] Normal B cells from a healthy adult were isolated from peripheral blood (PB; mean purity, 88.5%). PB was also obtained from 1 patient with XLA (P20) whose B-cell number was 0.09 in 1 μL whole blood and who was negative for sjKRECs ($<1.0 \times 10^2$ copies/μg DNA). Various numbers of normal B cells were serially added to 1 mL whole PB obtained from this patient with XLA. The B-cell–added XLA whole blood was then applied to filter papers, and 3 punches (3 mm in diameter) of dried blood spots were used for DNA extraction. At least 3 DNA samples containing the same B-cell concentrations (0.09-400 B cells/μL) were used for the real-time quantitative PCR of cjKRECs and sjKRECs. The percentages of the positive samples ($>1.0 \times 10^2$ copies/μg DNA) of cjKRECs and sjKRECs increased constantly

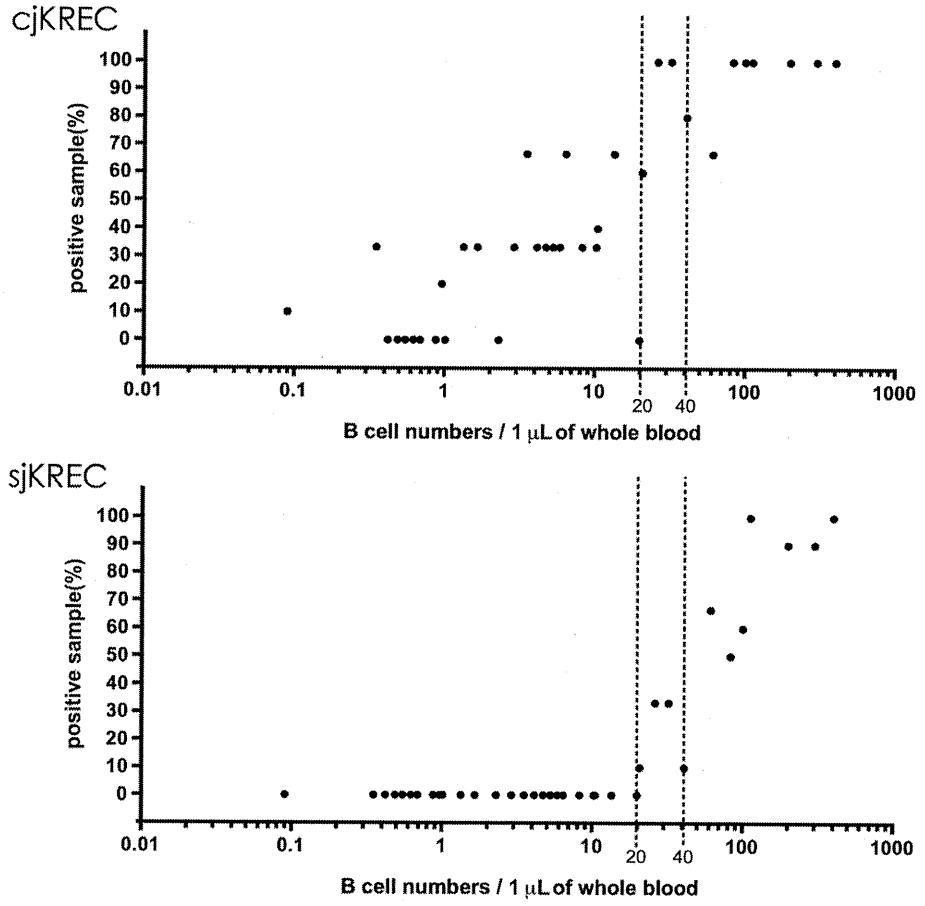

FIG 1. Sensitivity levels of cjKRECs and sjKRECs. Various numbers of purified normal B cells were serially added to whole PB from a patient with XLA (P20) to obtain B-cell–added XLA whole blood. cjKRECs and sjKRECs were measured in 3 to 10 samples of each concentration in triplicate. In all analyses, RNaseP (internal control) was positive ($2.3 \pm 0.2 \times 10^5$ copies/μg DNA). *X-axis,* B-cell numbers in 1 μL whole blood from a patient with XLA. *Y-axis,* Percentages of the KREC-positive results in the tests.

as the B-cell concentrations increased (Fig 1). None of the samples were positive for sjKRECs when the B-cell numbers were less than 20/μL, but cjKRECs were often positive. It has been reported that 90% of patients with XLA have less than 0.2% B cells in the PB at diagnosis.[1] Because peripheral lymphocyte numbers in neonates range from 1200 to 9800/μL,[8] the absolute B-cell numbers of 90% of patients with XLA are estimated to be 2.4 to 19.6/μL at the time of blood collection for Guthrie cards, although exact B-cell numbers of XLA in neonatal periods are not known at this moment. Because neonates are known to have fewer B cells than infants,[9] and we observed that B-cell numbers are constantly low in patients with XLA throughout infancy (Nakagawa, unpublished data, June 2010), which is consistent with the fact that BTK plays an essential role in B-cell maturation. It is likely that neonates with XLA also have severely decreased B cells. On the other hand, all samples obtained from 400 B cells/μL were positive for both cjKRECs and sjKRECs. We also observed that all healthy infants (1-11 months old; n = 15) were sjKREC-positive (Nakagawa, unpublished data, June 2010) and might have at least 600 B cells/μL whole blood.[9] From these data, it is assumed that at least 90% of patients with XLA are sjKREC-negative, and healthy neonates are positive for sjKRECs on neonatal Guthrie cards.

Next, we measured cjKRECs and sjKRECs in dried blood spots in filter papers or Guthrie cards from 30 patients with XLA and 5 patients with non-XLA and from 133 neonates born at the National Defense Medical College Hospital during this study period (August 2008 to October 2009) and 138 healthy subjects of various ages (1 month to 35 years old) to investigate the validity of this method. The levels of B cells of the patients ranged from 0.0% to 1.1% of total lymphocytes and 0.0 to 35.78/μL. IgG levels were 10 to 462 mg/dL (see this article's Tables E1 and E2 in the Online Repository at www.jacionline.org). Patients with leaky phenotypes[1,10] were included; 1 patient (P30) had more than 1% B cells and 34.22/μL total B cells, and 4 patients had more than 300 mg/dL serum IgG (P12, P30, P31, P33). All of the normal neonatal Guthrie cards were positive for both cjKRECs and sjKRECs ($7.2 \pm 0.7 \times 10^3$ and $4.8 \pm 0.6 \times 10^3$ copies/μg DNA, respectively). All healthy subjects of various ages were also positive for both cjKRECs and sjKRECs (Nakagawa, unpublished data, June 2010). In contrast, specimens from all 35 B-cell–deficient patients were sjKREC-negative ($<1.0 \times 10^2$ copies/μg DNA; Fig 2). All 5 patients with leaky phenotypes were also sjKREC-negative, which might be explained by the hypothesis that leaky B cells of patients with XLA are long-lived B cells that divided several times and have fewer sjKRECs than naive B cells.

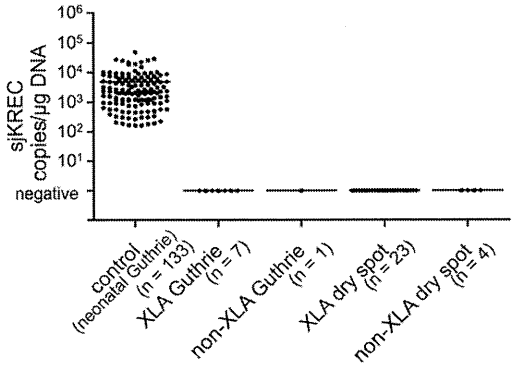

FIG 2. Copy numbers of sjKRECs measured in neonatal Guthrie cards or dried blood spots obtained from B-cell–deficient patients. On all samples from control, neonatal Guthrie cards (n = 133) were sjKREC-positive (4.8 ± 0.6 × 10^3 copies/μg DNA). B-cell–deficient patients were negative for sjKRECs in neonatal Guthrie cards (XLA, n = 7; non-XLA, n = 1) and dried blood spots (XLA, n = 23; non-XLA, n = 4).

One patient (P27) was positive for cjKRECs, but other patients were negative for it. *RPPH1* (internal control) was detectable at the same level as in normal controls in all samples.

These results indicate that sjKRECs are undetectable in XLA and non-XLA and suggest that measurement of sjKRECs in neonatal Guthrie cards has the potential for the use of newborn mass screening to identify neonates with early B-cell maturation defects. Greater numbers of neonatal Guthrie cards should be examined to confirm this potential, and the data obtained from dried blood spots on filter papers must be examined to prove that they truly reflect the data obtained from neonatal Guthrie cards. We should also examine whether screening can reduce the cost of treatment of the bacterial infections and chronic lung diseases in patients with XLA and non-XLA and increase the benefits for these patients. An anticipated pilot study using a large cohort of newborns must address these problems. We also found that T-cell–receptor excision circles and sjKRECs can be measured simultaneously on the same plate. Thus, a pilot study of neonatal screening for both T-cell and B-cell deficiencies could be performed simultaneously.

We thank the patients and their families who participated in this study. We also thank Ms Makiko Tanaka and Ms Kimiko Gasa for their skillful technical assistance and members of the Department of Obstetrics and Gynecology at the National Defense Medical College for collecting umbilical cord blood samples as well as Drs Wataru and Masuko Hirose. We are also indebted to Prof J. Patrick Barron, Chairman of the Department of International Medical Communications of Tokyo Medical University, for his *pro bono* linguistic review of this article.

Noriko Nakagawa, MD[a]
Kohsuke Imai, MD, PhD[a,b]
Hirokazu Kanegane, MD, PhD[c]
Hiroki Sato, MS[b]
Masafumi Yamada, MD, PhD[d]
Kensuke Kondoh, MD, PhD[e]
Satoshi Okada, MD, PhD[f]
Masao Kobayashi, MD, PhD[f]
Kazunaga Agematsu, MD, PhD[g]
Hidetoshi Takada, MD, PhD[h]
Noriko Mitsuiki, MD[i,j]
Koichi Oshima, MD[i,k]
Osamu Ohara, PhD[j]
Deepti Suri, MD[l]
Amit Rawat, MD[l]
Surjit Singh, MD[l]
Qiang Pan-Hammarström, MD, PhD[m]
Lennart Hammarström, MD, PhD[m]
Janine Reichenbach, MD[n]
Reinhard Seger, MD[n]
Tadashi Ariga, MD, PhD[d]
Toshiro Hara, MD, PhD[h]
Toshio Miyawaki, MD, PhD[c]
Shigeaki Nonoyama, MD, PhD[a]

From [a]the Department of Pediatrics, National Defense Medical College, and [b]the Department of Medical Informatics, National Defense Medical College Hospital, Saitama, Japan; [c]the Department of Pediatrics, University of Toyama, Toyama, Japan; [d]the Department of Pediatrics, Hokkaido University, Hokkaido, Japan; [e]the Department of Pediatrics, St Marianna University School of Medicine, Kanagawa, Japan; [f]the Department of Pediatrics, Hiroshima University, Hiroshima, Japan; [g]the Department of Pediatrics, Shinshu University, Nagano, Japan; [h]the Department of Pediatrics, Kyushu University, Fukuoka, Japan; [i]the Department of Pediatrics, Tokyo Medical and Dental University, Tokyo, Japan; [j]the Department of Human Genome Technology, Kazusa DNA Research Institute, Chiba, Japan; [k]the Department of Clinical Application, Center for iPS Cell Research and Application, Kyoto University, Kyoto, Japan; [l]the Advanced Pediatric Centre Post Graduate Institute of Medical Education and Research, Chandigarh, India; [m]the Division of Clinical Immunology, Department of Laboratory Medicine, Huddinge Hospital, Karolinska Institute, Stockholm, Sweden; and [n]the Department of Immunology/Hematology/BMT, University Children's Hospital Zurich, Zurich, Switzerland. E-mail: kimai@ndmc.ac.jp.

Supported in part by grants from the Ministry of Defense; the Ministry of Health, Labor, and Welfare; the Ministry of Education, Culture, Sports, Science and Technology; and the Kawano Masanori Foundation for Promotion of Pediatrics.

Disclosure of potential conflict of interest: The authors have declared that they have no conflict of interest.

REFERENCES

1. Conley ME, Broides A, Hernandez-Trujillo V, Howard V, Kanegane H, Miyawaki T, et al. Genetic analysis of patients with defects in early B-cell development. Immunol Rev 2005;203:216-34.
2. Kanegane H, Futatani T, Wang Y, Nomura K, Shinozaki K, Matsukura H, et al. Clinical and mutational characteristics of X-linked agammaglobulinemia and its carrier identified by flow cytometric assessment combined with genetic analysis. J Allergy Clin Immunol 2001;108:1012-20.
3. Plebani A, Soresina A, Rondelli R, Amato GM, Azzari C, Cardinale F, et al. Clinical, immunological, and molecular analysis in a large cohort of patients with X-linked agammaglobulinemia: an Italian multicenter study. Clin Immunol 2002;104:221-30.
4. Siminovitch KA, Bakhshi A, Goldman P, Korsmeyer SJ. A uniform deleting element mediates the loss of kappa genes in human B cells. Nature 1985;316: 260-2.
5. van Zelm MC, Szczepanski T, van der Burg M, van Dongen JJ. Replication history of B lymphocytes reveals homeostatic proliferation and extensive antigen-induced B cell expansion. J Exp Med 2007;204:645-55.
6. Eades-Perner AM, Gathmann B, Knerr V, Guzman D, Veit D, Kindle G, et al. ESID Registry Working Party. The European internet-based patient and research database for primary immunodeficiencies: results 2004-06. Clin Exp Immunol 2007; 147:306-12.
7. Morinishi Y, Imai K, Nakagawa N, Sato H, Horiuchi K, Ohtsuka Y, et al. Identification of severe combined immunodeficiency by T-cell receptor excision circles quantification using neonatal Guthrie cards. J Pediatr 2009;155:829-33.
8. Ozyurek E, Cetintas S, Ceylan T, Ogus E, Haberal A, Gurakan B, et al. Complete blood count parameters for healthy, small-for-gestational-age, full-term newborns. Clin Lab Haematol 2006;28:97-104.
9. Comans-Bitter WM, de Groot R, van den Beemd R, Neijens HJ, Hop WC, Groeneveld K, et al. Immunophenotyping of blood lymphocytes in childhood: reference values for lymphocyte subpopulations. J Pediatr 1997;130:388-93.
10. Kaneko H, Kawamoto N, Asano T, Mabuchi Y, Horikoshi H, Teramoto T, et al. Leaky phenotype of X-linked agammaglobulinaemia in a Japanese family. Clin Exp Immunol 2005;140:520-3.

Available online March 11, 2011.
doi:10.1016/j.jaci.2011.01.052

TABLE E1. Characteristics of patients with XLA

Patient no.	Unique patient no.	Age (y)	Sex	Serum Ig (mg/dL)			$CD19^+$		*BTK* mutation			Source	
				IgG	IgA	IgM	% Lymph	/μL	Genomic DNA	cDNA	Amino acid	Guthrie	Dry spot
P1	670	0	M	87	<6	10	0.21	12.99	29269G>T	1178-1G>T	Splice acceptor defect	x	
P2	718	0	M	215	<10	<10	0.07	7.04	11593_11594 insA	144_145insA	Arg49 frameshift	x	
P3	722	0	M	80	<1	1	<1.00	NA	25644C>T	763C>T	Arg255X	x	
P4	727	8	M	295	59	57	0.11	3.52	29269G>T	1178-1G>T	Splice acceptor defect		x
P5	732	34	M	1140*	<6	8	0.02	0.24	11631T>A	182T>A	Ile61Asn		x
P6	811	24	M	458*	0	13	0.50	5.32	23570T>G	426T>G	Tyr142X		x
P7	813	18	M	628*	109	6	0.60	6.87	23570T>G	426T>G	Tyr142X		x
P8	814	19	M	260	0	NA	0.20	3.01	16180C>T	344C>T	Ser115Phe		x
P9	815	13	M	600*	<10	<5	0.08	1.72	11590G>T	142-1G>T	Splice acceptor defect		x
P10	816	11	M	12	0	5	0.00	0.00	150kb deletion of *BTK, TIMM8A, TAF7L, DRP2*				x
P11	817	10	M	10	2	24	0.80	35.78	36288C>T	1928C>T	Thr643Ile		x
P12	824	13	M	462	6	27	0.41	14.49	27518C>A	895-11C>A	Splice acceptor defect		x
P13	834	5	M	<237	<37	43	0.00	0.00	25715_26210del	776+57_839+73del	Exon 9 deletion		x
P14	838	21	M	<50	<5	7	0.00	0.00	31596G>C	1631+1G>C	Splice donor defect		x
P15	839	16	M	604*	<1	<2	0.04	0.66	31596G>C	1631+1G>C	Splice donor defect		x
P16	847	11	M	698*	26	11	0.08	1.86	25536delG	655delG	Val219 frameshift		x
P17	877	14	M	20	19	8	0.21	NA	32357T>C	1750+2T>C	Splice donor defect		x
P18	880	5	M	233	39	41	0.06	NA	10941-?_14592+?del	1-?_240+?del	Exon 1-3 deletion		x
P19	888	8	M	<212	<37	150	0.15	6.60	11023G>A	83G>A	Arg28His		x
P20	891	21	M	195	<6	37	0.02	0.09	32243C>G	1638C>G	Cys502Trp		x
P21	958	0	M	<50	<10	9	0.80	27.14	31544_31547 delGTTT	1580_1583del GTTT	Cys527 frameshift		x
P22	701	2	M	115	<2	4	0.09	1.99	16172C>A	336C>A	Tyr112X		x
P23	911	0	M	<10	<6	<4	0.00	0.00	29955A>C	1350-2A>C	Splice acceptor defect	x	
P24	937	0	M	60	<2	58	0.00	0.00	11022C>T	82C>T	Arg28Cys	x	
P25	938	0	M	<20	<4	<6	0.00	0.00	36269-?_36778+?del	1909-?_2418+?del	Exon 19 deletion	x	
P26	939	0	M	60	<2	22	0.00	0.00	11022C>T	82C>T	Arg28Cys	x	
P27	890	12	M	<237	<37	<20	0.03	NA	36261G>A	1909-8G>A	Splice acceptor defect		x
P28	944	6	M	12	<1	1	0.02	NA	36281C>T	1921C>T	Arg641Cys		x
P29	948	5	M	<237	<37	<20	0.01	0.70	36261G>A	1909-8G>A	Splice acceptor defect		x
P30	1053	5	M	386	5	113	1.10	34.22	32259A>C	1654A>C	Thr552Pro		x

Age, Age at analysis of KRECs; *$CD19^+$ % Lymph,* CD19-positive cell percentage in lymphocytes; *$CD19^+$ /μL,* CD19-positive cell number in 1 μL whole peripheral blood; *M,* male; *NA,* not available; *Serum Ig,* serum levels of immunoglobulins at diagnosis.

BTK mutation's reference sequences are NCBI NC_000023.9, NM_000061.2, and NP_000052.1.

*Trough level during intravenous immunoglobulin therapy.

TABLE E2. Characteristics of patients with non-XLA

				Serum Ig (mg/dL)			$CD19^+$			Source	
Patient no.	Unique patient no.	Age (y)	Sex	IgG	IgA	IgM	% Lymph	/μL	*BTK* mutation	Guthrie	Dry spot
P31	596	4	F	386	<6	6	0.42	21.27	Normal		x
P32	719	0	F	<50	<5	<5	0.00	0.00	Normal	x	
P33	835	8	M	311	323	20	0.09	1.88	Normal		x
P34	915	0	M	<212	<37	<20	0.00	0.00	Normal		x
P35	947	0	M	<21	<37	<39	0.00	0.00	Normal		x

Age, Age at analysis of KRECs; *$CD19^+$ % Lymph,* CD19-positive cell percentage in lymphocytes; *$CD19^+$ /μL,* CD19-positive cell number in 1 μL whole peripheral blood; *F,* female; *M,* male; *Serum Ig,* serum levels of immunoglobulins at diagnosis.

OPEN ACCESS Freely available online

PLoS one

A Novel Serum-Free Monolayer Culture for Orderly Hematopoietic Differentiation of Human Pluripotent Cells via Mesodermal Progenitors

Akira Niwa[1,2], Toshio Heike[2], Katsutsugu Umeda[2,4], Koichi Oshima[1], Itaru Kato[1,2], Hiromi Sakai[5], Hirofumi Suemori[3], Tatsutoshi Nakahata[1,2], Megumu K. Saito[1,2]*

1 Clinical Application Department, Center for iPS Cell Research and Application, Kyoto University, Kyoto, Japan, **2** Department of Pediatrics, Graduate School of Medicine, Kyoto University, Kyoto, Japan, **3** Laboratory of Embryonic Stem Cell Research, Stem Cell Research Center, Institute for Frontier Medical Sciences, Kyoto University, Kyoto, Japan, **4** Institute of Molecular Medicine, University of Texas Health Science Center, Houston, Texas, United States of America, **5** Waseda Bioscience Research Institute in Helios, Singapore

Abstract

Elucidating the *in vitro* differentiation of human embryonic stem (ES) and induced pluripotent stem (iPS) cells is important for understanding both normal and pathological hematopoietic development *in vivo*. For this purpose, a robust and simple hematopoietic differentiation system that can faithfully trace *in vivo* hematopoiesis is necessary. In this study, we established a novel serum-free monolayer culture that can trace the *in vivo* hematopoietic pathway from ES/iPS cells to functional definitive blood cells via mesodermal progenitors. Stepwise tuning of exogenous cytokine cocktails induced the hematopoietic mesodermal progenitors via primitive streak cells. These progenitors were then differentiated into various cell lineages depending on the hematopoietic cytokines present. Moreover, single cell deposition assay revealed that common bipotential hemoangiogenic progenitors were induced in our culture. Our system provides a new, robust, and simple method for investigating the mechanisms of mesodermal and hematopoietic differentiation.

Citation: Niwa A, Heike T, Umeda K, Oshima K, Kato I, et al. (2011) A Novel Serum-Free Monolayer Culture for Orderly Hematopoietic Differentiation of Human Pluripotent Cells via Mesodermal Progenitors. PLoS ONE 6(7): e22261. doi:10.1371/journal.pone.0022261

Editor: Dan Kaufman, University of Minnesota, United States of America

Received January 4, 2011; **Accepted** June 18, 2011; **Published** July 27, 2011

Funding: This work was supported by grants from the Ministry of Education, Culture, Sports, Science, and Technology of Japan (#22790979). The funders had no role in study design, data collection and analysis, decision to publish, or preparation of the manuscript.

Competing Interests: The authors have declared that no competing interests exist.

* E-mail: msaito@kuhp.kyoto-u.ac.jp

Introduction

Because of pluripotency and self-renewal, human embryonic stem (ES) cells and induced pluripotent stem (iPS) cells are potential cell sources for regenerative medicine and other clinical applications, such as cell therapies, drug screening, toxicology, and investigation of disease mechanisms [1,2,3]. iPS cells are reprogrammed somatic cells with ES cell-like characteristics that are generated by introducing certain combinations of genes, proteins, or small molecules into the original cells [4,5,6,7]. Patient-derived iPS cells have facilitated individualized regenerative medicine without immunological or ethical concerns. Moreover, patient- or disease-specific iPS cells are an important resource for unraveling human hematological disorders. However, for this purpose, a robust and simple hematopoietic differentiation system that can reliably mimic in vivo hematopoiesis is necessary.

Mesodermal and hematopoietic differentiation is a dynamic event associated with changes in both the location and phenotype of cells [8,9,10,11]. Some primitive streak (PS) cells appearing just after gastrulation form the mesoderm, and a subset of mesodermal cells differentiate into hematopoietic cell lineages [9,12,13,14,15,16]. Previous studies have accumulated evidence on these embryonic developmental pathways.

The leading methods of blood cell induction from ES/iPS cells employ 2 different systems: monolayer animal-derived stromal cell coculture and 3-dimensional embryoid body (EB) formation. Both methods can produce hematopoietic cells from mesodermal progenitors, and combinations of cytokines can control, to some extent, the specific lineage commitment [1,2,17,18,19,20,21,22,23,24,25,26,27,28]. In the former method, a previous study showed that OP9 stromal cells, which are derived from the bone marrow of osteopetrotic mice, augment the survival of human ES cell-derived hematopoietic progenitors [29]. However, as the stromal cell condition controls the robustness of the system, it can be relatively unstable. Furthermore, the induction of hematopoietic cells from human pluripotent cells on murine-derived cells is less efficient than that from mice cells.

In EB-based methods, hematopoietic cells emerge from specific areas positive for endothelial markers such as CD31 [30,31,32]. Through these methods, previous studies have generated a list of landmark genes for each developmental stage, such as *T* and *KDR* genes for the PS and mesodermal cells, respectively [12,16,17,18,25,28,33,34,35,36], and also have emphasized appropriate developmental conditions consisting of specific microenvironments, signal gradients, and cytokines given in suitable combinations with appropriate timing. For robust and reproducible specification to myelomonocytic lineages of cells, some recent studies have converted to serum-independent culture by using EB formation [37]. However, the difficulty in applying 3-dimensional location information inside EBs prevents substantial increases in

hematopoietic specification efficacy. Additionally, the sphere-like structure of the EB complicates tracking and determination of hematopoietic–stromal cell interactions.

To overcome these issues, we established a novel serum-free monolayer hematopoietic cell differentiation system from human ES and iPS cells. Although there are no reports describing the shift of human ES/iPS cells from primitive to definitive erythropoiesis in a monolayer xeno-cell-free condition, our system can trace the in vitro differentiation of human ES/iPS cells into multiple lineages of definitive blood cells, such as functional erythrocytes and neutrophils. Hematopoietic cells arise via an orderly developmental pathway that includes PS cells, mesoderm, and primitive hematopoiesis.

Materials and Methods

Maintenance of human ES/iPS cells in serum-free condition

Experiments were carried out with the human ES cell lines KhES-1 and KhES-3 (kindly provided by Norio Nakatsuji) and iPS cell lines 201B7 and 253G4 (kindly provided by Shinya Yamanaka). Stable derivatives of ES cells carrying the transgene for green fluorescent protein (GFP) after CAG promoter were also used [38,39]. The ES/iPS cells were maintained on a tissue culture dish (#353004; Becton-Dickinson, Franklin Lakes, NJ) coated with growth factor-reduced Matrigel (#354230; Becton-Dickinson) in mTeSR1 serum-free medium (#05850; STEMCELL Technologies, Vancouver, BC, Canada). The medium was replaced everyday. Passage was performed according to the manufacturer's protocol.

Differentiation of ES/iPS cells

First, undifferentiated ES/iPS cell colonies were prepared at the density of less than 5 colonies per well of a 6-well tissue culture plate (#353046; Becton-Dickinson). When individual colony grew up to approximately 500 μm in diameter, mTeSR1 maintenance medium was replaced by Stemline II serum-free medium (#S0192; Sigma-Aldrich, St. Louis, MO) supplemented with Insulin-Transferrin-Selenium-X Supplement (ITS) (#51500-056; Invitrogen, Carlsbad, CA). This day was defined as day 0 of differentiation. BMP4 (#314-BP-010; R&D Systems, Minneapolis, MN) was added for first 4 days and replaced by $VEGF_{165}$ (#293-VE-050; R&D Systems) and SCF (#255-SC-050; R&D Systems) on day 4. On day 6, the cytokines were again replaced by the haematopoietic cocktail described in the result section. Concentration of each cytokine was as follows: 20 ng/mL BMP4, 40 ng/mL $VEGF_{165}$, 50 ng/mL SCF, 10 ng/mL TPO (#288-TPN-025; R&D Systems), 50 ng/mL IL3 (#203-IL-050; R&D Systems), 50 ng/mL Flt-3 ligand (#308-FK-025; R&D Systems), 50 ng/mL G-CSF (#214-CS-025; R&D Systems), 50 ng/mL complex of IL-6 and soluble IL-6 receptor (FP6) (kindly provided by Kyowa Hakko Kirin Co., Ltd., Tokyo, Japan) and 5 IU/mL EPO (#329871; EMD Biosciences, San Diego, CA). Thereafter, the medium was changed every 5 days.

Antibodies

The primary murine anti-human monoclonal antibodies used for flow cytometric (FCM) analysis are as follows: PE-conjugated anti-SSEA-4 (#330405; BioLegend, San Diego, CA), Alexa Fluor® 647-conjugated anti-TRA-1-60 (#560122; Becton-Dickinson), biotin-conjugated anti-CD140a (#323503; Biolegend), Alexa Fluor® 647-conjugated anti-KDR (#338909; BioLegend), PE-conjugated anti-CXCR4 (#555974; Becton-Dickinson), PE-conjugated anti-CD117 (#313203; BioLegend), PE-conjugated CD34 (#A07776; Beckman Coulter, Brea, CA), FITC-conjugated CD43 (#560978; Becton-Dickinson), and APC-conjugated CD45 (#IM2473; Beckman Coulter). A streptavidin-PE (#554061; Becton Dickinson) was used as secondary antibody against biotin-conjugated primary antibody. The primary antibodies used to immunostain the colonies and floating blood cells included anti-human Oct3/4 (#611203; Becton-Dickinson), T (#sc-101164; Santa Cruz Biotechnology, Santa Cruz, CA), KDR (#MAB3571; R&D Systems), VE-Cadherin (#AF938; R&D Systems), and rabbit anti-pan-human Hb (#0855129; MP Biomedicals, Solon, OH). FITC-conjugated donkey anti-rat antibodies and Cy3-conjugated goat anti-mouse antibodies (Jackson ImmunoResearch Laboratories, Inc., West Grove, PA) were used as secondary antibodies.

Cytostaining

Floating cells were centrifuged onto glass slides by using a Shandon Cytospin 4 Cytocentrifuge (Thermo, Pittsburgh, PA) and analysed by microscopy after staining with May–Giemsa or myeloperoxidase. For immunofluorescence staining, cells fixed with 4% paraformaldehyde were first permeabilized with phosphate-buffered saline containing 5% skimmed milk (Becton–Dickinson) and 0.1% Triton X-100 and then incubated with primary antibodies, followed by incubation with FITC or Cy3-conjugated secondary antibodies. Nuclei were counterstained with 4,6-diamidino-2-phenylindole (DAPI) (Sigma-Aldrich).

Flow cytometric analysis

The adherent cells were treated with Dispase (#354235; Becton-Dickinson) and harvested by gently scraping the culture dish. Aggregated cell structure was chopped by a pair of scissors, processed by GentleMACS (Milteny Biotec, Germany) and then dispersed by 40-μm strainers (#2340; Becton-Dickinson) before staining with antibodies. Dead cells were excluded by DAPI staining. Samples were analysed using a MACSQuant (Milteny Biotec) and FlowJo software (Thermo). Cell sorting was performed using a FACSVantage or FACSAria (Becton–Dickinson).

RNA extraction and real-time quantitative PCR analysis

RNA samples were prepared using silica gel membrane-based spin-columns (RNeasy Mini-KitTM; Qiagen, Valencia, CA) and subjected to reverse transcription (RT) with a Sensiscript-RT Kit (Qiagen). All procedures were performed according to the manufacturer's instructions. For real-time quantitative PCR, primers and the fluorogenic probes were designed and selected according to Roche Universal Primer library software (Roche Diagnostics) and MGB probe system (Applied Biosystems, Carlsbad, CA). The instrument used was the Applied Biosystems ABIPrism 7900HT sequence detection system, and the software for data collection and analysis was SDS2.3. A GAPDH RNA probe (Hs00266705_g1) was used to normalise the data.

Clonogenic colony-forming assay

At the indicated days of culture, from days 6 through 25, the adherent cells were treated with dispase and harvested. They were incubated in a new tissue-culture dish (#3003, Becton–Dickinson) for 10 min to eliminate adherent non-haematopoietic cells [40]. Floating cells were collected and dispersed by 40-μm strainers. After dead cells were eliminated by labeling with Dead-Cert Nanoparticles (#DC-001, ImmunoSolv, Edinburgh, UK), live hematopoietic cells were cultured at a concentration of 1×10^3 (for counting CFU-G) or 10^4 (for counting CFU-Mix, BFU-E, and CFU-GM) cells/ml in 35-mm petri dishes (#1008; Becton-Dickinson) using

1 ml/dish of MethoCult GF+ semisolid medium (#4435; STEMCELL Technologies) as previously described. Colonies were counted after 14–21 days of incubation, and colony types were determined according to the criteria described previously [41,42,43] by in situ observation using an inverted microscope. The abbreviations used for the clonogenic progenitor cells are as follows: CFU-Mix, mixed colony-forming units; BFU-E, erythroid burst-forming units; CFU-GM, granulocyte–macrophage colony-forming units; and CFU-G, granulocyte colony-forming units.

Single-cell deposition assay

The single-cell deposition assay was performed as described previously [17,18,28]. In brief, single sorted cells were deposited in individual wells of 96-well plates with confluent OP9 layers and cultured for 14 days. Wells were scored by morphological observation for hematopoietic colony detection and stained with anti-vascular endothelial cadherin (VE-cadherin) antibodies for endothelial lineage detection.

Chemotaxis assay

Chemotaxis assay was performed with modified Boyden chamber method using 3.0-μm pore size cell culture inserts (Becton Dickinson). In brief, 5×10^4 cells harvested from floating cell fraction at day 25 were added to the upper chamber and induced to migrate towards the lower chamber containing 10 nM formyl-Met-Leu-Phe (fMLP; Sigma-Aldrich) for 4 hours at 37°C. After incubation, the cells in the lower chamber were collected and counted using a MACSQuant flow cytometer (Miltenyi Biotec). For quantitative analysis, equivalent amount of 6-μm beads (Becton Dickinson) were added to each FCM sample, and the cell numbers were determined by measuring the ratio of cells to beads.

Phagocytosis and detection of reactive oxygen species

Phagocytosis and production of reactive oxygen species were detected by chemiluminescent microspheres (luminol-binding carboxyl hydrophilic microspheres; TORAY, Tokyo, Japan) as described previously [44]. In brief, 2×10^4 floating cells were suspended in 50 μL of the reaction buffer (HBSS containing 20 mM *N*-2-hydroxyethylpiperazine-*N*-2-ethanesulfonic acid (HEPES)) per tube. To activate the system, 5 μl chemiluminescent microspheres were added, and light emission was recorded continuously using a luminometer (TD-20/20; Turner Designs, Sunnyvale, CA). During the measurement, samples were kept at 37°C. To inhibit the reaction, 1.75 μg of cytochalasin B (Sigma-Aldrich) was added to the samples.

Measurement of oxygen-binding ability

Floating blood cells derived from KhES-1 and 253G4 strains were harvested on day 32 of differentiation (with erythropoietic cytokine cocktail). Oxygen dissociation curves for hemoglobin were measured using a Hemox-Analyzer (TCS Scientific Corporation, New Hope, PA) as previously reported [45,46].

Results

Stepwise generation of functional hematopoietic cells from human ES/iPS cells in the serum-free monolayer culture without animal-derived stromal cells

To assess the differentiation activity of each human ES/iPS cell line with high reproducibility, we used a chemically defined medium in the monolayer differentiation culture and succeeded in inducing various blood cells, including erythrocytes and neutrophils (Figure 1a). To present the developmental process from human ES/iPS cells to blood cells in an orderly manner, we divided the entire process into 3 steps: (1) initial differentiation into PS cells, (2) induction of the hematopoietic mesoderm (Movie S1), and (3) commitment to the hematopoietic lineages (Movie S2).

Step 1: Induction of PS-like cells from undifferentiated human ES/iPS cells with BMP4 (days 0–4). First, we examined the efficacy of initial progression from undifferentiated pluripotent cells (KhES-1) into PS-like cells according to the expression of representative marker genes, such as *T* and *Mixl1* (Figure 1b), and the change in morphology (Figure 1c). Without cytokines, these genes were only slightly upregulated during the first 4 days. However, when 40 ng/mL BMP4 was added to the culture, the expression levels of these genes increased, which is compatible with previous reports on the importance of BMP4 in mesodermal/endodermal differentiation via PS during early embryogenesis (Figure 1b). Further, transcription levels of the undifferentiated marker *Nanog* decreased. During this period, the colonies showed substantial morphological changes at the margins, and cell density decreased and cell contact diminished (Movie S1, Figure 1c). Immunohistochemical staining assays confirmed the upregulation of T and the lateral mesodermal marker, KDR, and downregulation of Oct3/4 (Figure 1c). However, regarding ectodermal commitment, the representative marker gene *Sox1* was hardly detected on day 4 in the presence of BMP4 (Figure 1b).

To assess the role of BMP4 in this step, we analyzed the differentiation efficacy of individual ES (KhES-1 and KhES-3) and iPS (201B7 and 253G4) cell strains with various concentrations of BMP4 in the presence or absence of its inhibitor, Noggin. As shown in Figure 1d, *T* gene expression was upregulated by BMP4 dose-dependently up to 20 ng/mL and was almost completely suppressed by the BMP4 inhibitor, Noggin, in both ES and iPS cells. This suggested that BMP4 was critical at this stage. From these results, we used BMP4 at 20 ng/mL concentration in subsequent experiments.

We also assayed the expression of several cell surface protein markers in this step (Figure 1e). On day 4, undifferentiated cell markers (TRA-1-60 and SSEA4) were downregulated, whereas paraxial and lateral mesoderm cell markers (CD140a and KDR) and markers for mesodermal and hematopoietic progenitors (CXCR4 and CD117) were upregulated. The early-phase hematopoietic-committed cell markers (CD34 and CD43) were still negative at this stage. Similar results were obtained for both ES and iPS cells (data not shown), suggesting that our system initiated paraxial and lateral mesodermal differentiation from pluripotent stem cells during Step 1 [33].

Step 2: Generation of $KDR^+CD34^+CD45^-$ progenitors with VEGF and SCF (days 4–6). Our previous studies of primate ES cells demonstrated that $KDR^+CD34^+CD45^-$ mesodermal progenitors derived in a VEGF-containing culture on OP9 stromal cells included hematopoietic progenitors [17,18]. Therefore, we used this data to induce these progenitors in our culture system. Considering the partial expression of KDR and CD117 during the first step, we replaced BMP4 with 40 ng/mL $VEGF_{165}$ (ligand for KDR) and 50 ng/mL SCF (ligand for CD117) on day 4 to accelerate selective differentiation to the lateral mesoderm with hematopoietic activities (Figure 1a).

During the next 2 days, the colonies exhibited 2 distinct regions: a plateau-like central area with stratified components and a surrounding area with monolayer cells (Movie S1, Figure 1c). On day 6, the mRNA expression pattern indicated the dominance of mesodermal cells rather than endodermal or ectodermal lineages

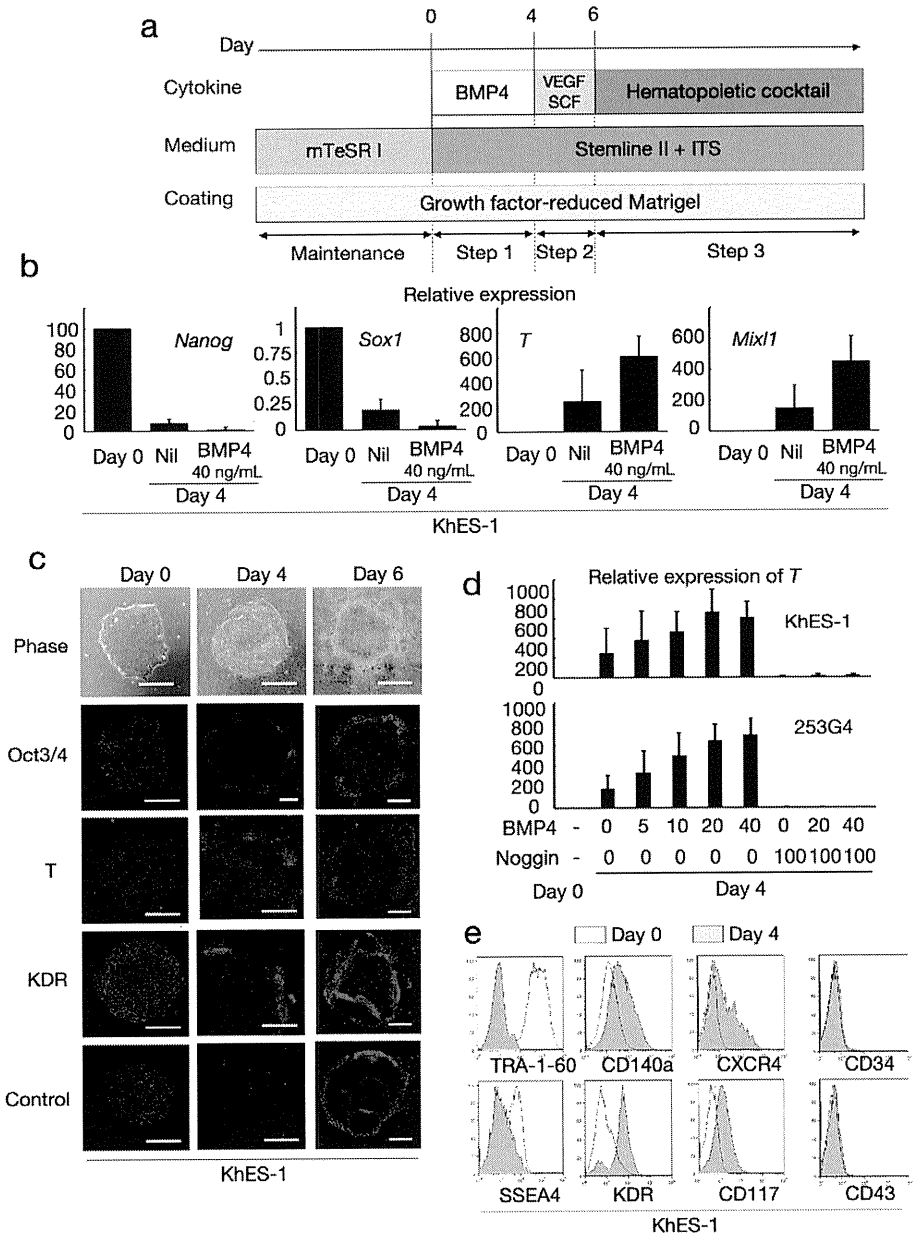

Figure 1. Blood cell induction from pluripotent stem cells starts with commitment into primitive streak. a. A schema of stepwise haematopoietic differentiation of human ES/iPS cells. **b.** Gene expression analysis of colonies at the beginning of differentiation (day 0) and the end of step 1 (day 4) with/without 40 ng/mL BMP4. Data from KhES-1 are shown as representative. **c.** Phase contrast microscopies and immunofluorescence staining of colonies during initial differentiation. Data from KhES-1 are shown as representative. **d.** Relative expression of *T* at day 4 of differentiation with different combinations of BMP4 and its inhibitor Noggin. Where shown, bars represent standard deviation of the mean of three independent experiments; Scale bars, 500 μm. Data from KhES-1 and 253G4 strains are shown as representative. **e.** Flow cytometric analysis of differentiating cells on day 4, indicating the down-regulation of immature cell markers and up-regulation of differentiated progenitor markers. Data from KhES-1 are shown as representative.
doi:10.1371/journal.pone.0022261.g001

(Figure 2a), and flow cytometric (FCM) analysis demonstrated the emergence of new cell fractions that were positive for KDR, CD117, CXCR4, and CD34 but negative for CD140a, CD43, and CD45 (Figure 2b). Our system robustly supports mesodermal induction from both ES and iPS cells, despite differences in efficacy among cell strains (Figure 2c).

Further, immunohistochemical staining for KDR indicated an uneven distribution of KDR^+ cells at the marginal zone of the plateau area (Figure 1c), suggesting that differentiation polarity within the colonies resulted in site-specific emergence of putative hematopoietic mesodermal progenitors.

Step 3: Production of functional blood cells dependent on cytokine cocktails (day 6 onward). On day 6, we changed the culture medium to another chemically defined medium containing hematopoietic cytokines (Figure 1a). To achieve lineage-directed differentiation, we used 2 combinations of cytokines: a myeloid-

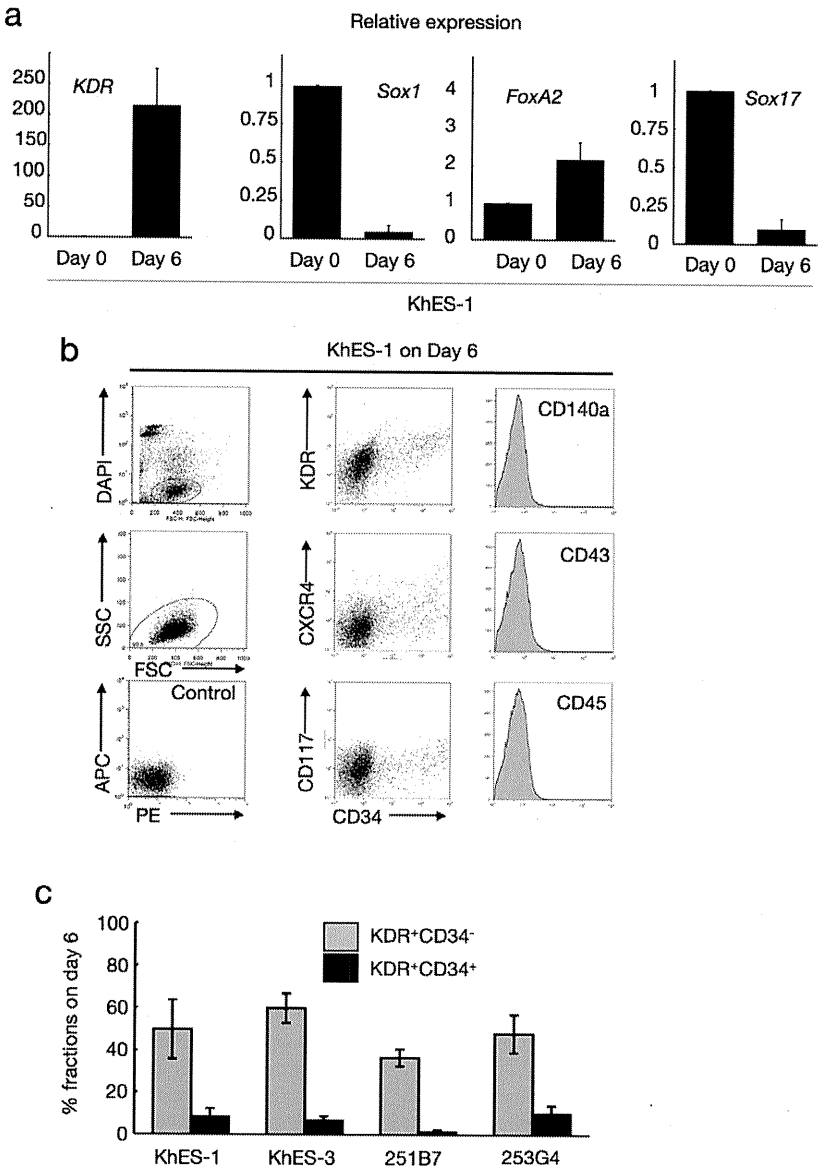

Figure 2. Characterization of cells during initial differentiation with lineage-specific marker expression. a. Expression analysis of lineage-specific marker genes at the beginning of differentiation (day 0) and the end of step 2 (day 6). Bars represent standard deviation of the mean of three independent experiments. Data from KhES-1 are shown as representative. **b.** The development of progenitors on day 6 positive for lateral mesoderm markers but negative for paraxial mesoderm and haematopoietic cell markers. Leftmost column shows the gating strategy for eliminating dead cells and debris. Data from KhES-1 are shown as representative. c. Efficacy of inducing $KDR^{+}CD34^{+\text{ or }-}$ mesodermal progenitors from each two lines of human ES cells and iPS cells. Bars represent standard deviation of the mean of three independent experiments.
doi:10.1371/journal.pone.0022261.g002

induction cocktail containing SCF, TPO, IL3, FLT-3 ligand, and G-CSF; and an erythropoietic-differentiation cocktail containing SCF, TPO, IL3, FP6, and EPO.

Regardless of the cocktails, the colonies first exhibited a rosary-like appearance, with small sac-like structures aligned along the margins of the plateau areas, and grew for several days (Figure 3a, left panel). Hematopoietic cell clusters emerged from the edge of these structures on days 10–12, followed by the appearance of floating blood cells a few days later, which increased thereafter; hematopoietic clusters grew in size and number, and some exhibited areas with a cobblestone-like appearance (Figure 3a, right 3 panels; Movie S2). When fresh medium with the cytokines was supplied every 5 days, blood cell production was observed in both ES and iPS cell experiments until day 50 of differentiation, whereas few hematopoietic cells appeared without the cytokines (data not shown).

As expected, the myeloid-induction cocktail induced myelomonocytic lineages predominantly positive for CD45. Blood cells harvested on day 30 exhibited morphology compatible with myelomonocytic precursors and mature neutrophils, and displayed positive myeloperoxidase staining (Figure 3b). On the other hand, the erythropoietic-differentiation cocktail yielded cell lineages that included hemoglobin-positive (Hb^{+}) erythroid cells and $CD41^{+}$ megakaryocytes (Figure 3b). In the KhES-1 strain (3.5 [standard deviation (SD) = 1.5] undifferentiated colonies 250 μmm in diameter were initially plated in individual wells of 6-well plates

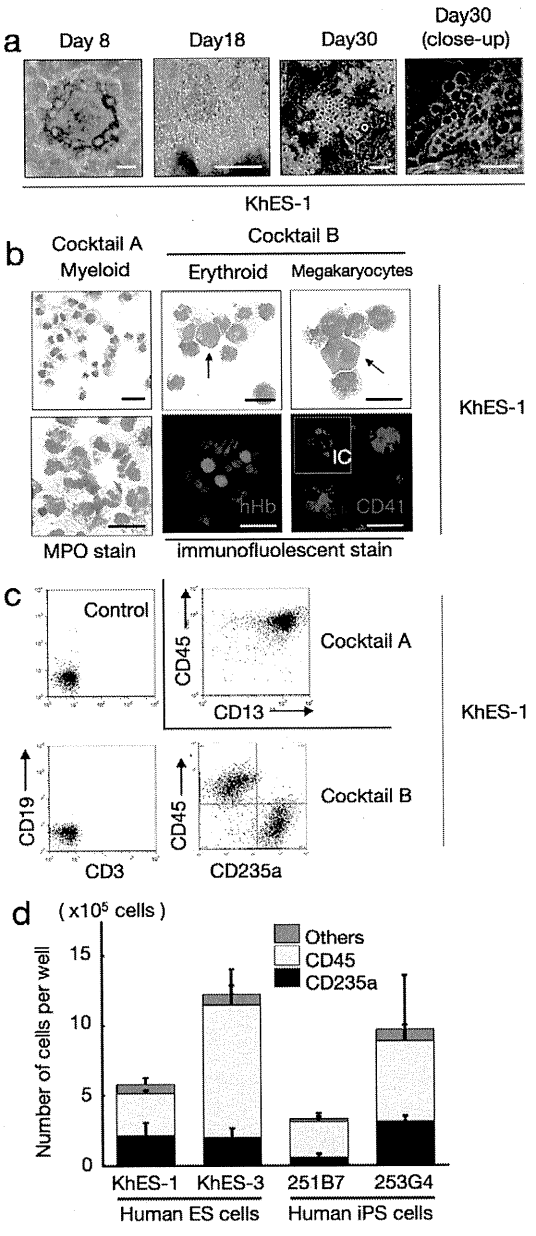

Figure 3. Human ES/iPS cell-derived haematopoiesis in a monolayer culture free from animal serum or stromal cells. a. Sequential phase contrast pictures showing haematopoietic development. Scale bars, 500 μm (left two panels) and 100 μm (right two panels). Data from KhES-1 are shown as representative. **b.** Floating cells harvested on day 30 showing various lineages of haematopoietic cells; MPO-positive myeloid lineage cells (leftmost panels), pan-human Hb-positive erythroid lineage cells (centre panels), and CD41-positive megakaryocytes (rightmost panels). Scale bars, 100 μm. Data from KhES-1 are shown as representative. **c.** Expression of lineage-specific antigens on floating cells harvested on day 30; Myeloid lineages (CD13 and CD45), erythroid lineages (CD235a), T cells (CD3), and B cells (CD19). Data from KhES-1 are shown as representative. **d.** Numbers and fraction of blood cells induced from each two lines of human ES cells and iPS cells. Bars represent standard deviation of the mean of three independent experiments.
doi:10.1371/journal.pone.0022261.g003

at the start of differentiation), counting and FCM analysis of harvested blood cells on day 30 revealed the existence of 7.7×10^5 (SD = 2.3×10^5) different cell lineages per well, including 36.0% (SD = 6.4%) $CD235a^+$ erythroid and 53.2% (SD = 9.4%) $CD45^+$ myelomonocytic lineages, but no lymphoid lineage cells (Figure 3c). Although the differentiation efficacy and lineage distribution depend not only on the cytokines but also on the cell strains, the data indicates that human ES and iPS cells develop into various lineages of hematopoietic cells, robustly and orderly, in our novel monolayer culture system without xeno-derived serum or stromal cells (Figure 3d).

ES/iPS cell-derived hematopoietic cells have similar potential to in vivo-derived blood cells in function

Considering the use of ES/iPS cell-derived hematopoiesis for various clinical and research applications, it is important to confirm the function of the generated blood cells. Neutrophils derived with the myeloid-induction cocktail exhibited migration activity in response to the chemoattractant fMLP (Figure 4a) and phagosome-dependent reactive oxygen production, which was inhibited by the phagosome destruction agent, cytochalasin B (Figure 4b). On the other hand, erythroid lineage cells derived with the erythropoietic-differentiation cocktail (harvested on day 32 of differentiation) exhibited an oxygen dissociation curve that was similar, despite being slightly left-shifted, to those obtained with adult and cord blood cells (Figure 4c). These data indicate that our culture facilitates robust and orderly development of human ES and iPS cells into functional hematopoietic cells with similar potential to in vivo-derived blood cells.

Clonogenic hematopoietic development from human ES/iPS cell-derived progenitors

The human hematopoietic system is a hierarchy of various component cells from stem or progenitor cells to terminally differentiated cells. For example, $CD34^+$ cells in umbilical cord blood or bone marrow contain putative hematopoietic stem cells and are used as a source of stem cell transplantation. The identification and proliferation of such cells in vitro have been of great interest in medical science research.

To assess the potential of our system for supporting generated immature stem or progenitor cells, we evaluated the colony-forming ability of the cultivated hematopoietic progenitors in the system. Accordingly, the cells were cultured with SCF, TPO, IL3, FLT-3 ligand, and FP6. In these conditions, $CD34^+CD45^+$ hematopoietic cells existed up to day 25, indicating that the immature hematopoietic cells can be maintained in our serum-free culture (Figure 5a).

We harvested adherent blood cells from the previously described culture and transferred them into a methylcellulose-containing medium to perform colony-forming assays with SCF, TPO, IL3, G-CSF, and EPO. As shown in Figure 5b and c, CFU-Mix, BFU-E, CFU-GM, and CFU-G colonies developed from plated cells. The total number of colonies increased dramatically from day 6 to day 10, then gradually increased until day 15 and decreased thereafter. CFU-Mix and BFU-E colonies were mainly observed until day 15 and were thereafter replaced by CFU-GM and CFU-G colonies. Similar tendencies were observed in both ES and iPS cells. These results suggest that our culture system can incubate multipotent hematopoietic stem or progenitor cells over a period of time.

Identification of $KDR^+CD34^+CD45^-$ bipotential hemoangiogenic progenitors derived in serum-free conditions

During embryogenesis, hematopoietic development is closely associated with endothelial lineage commitment [47,48], and

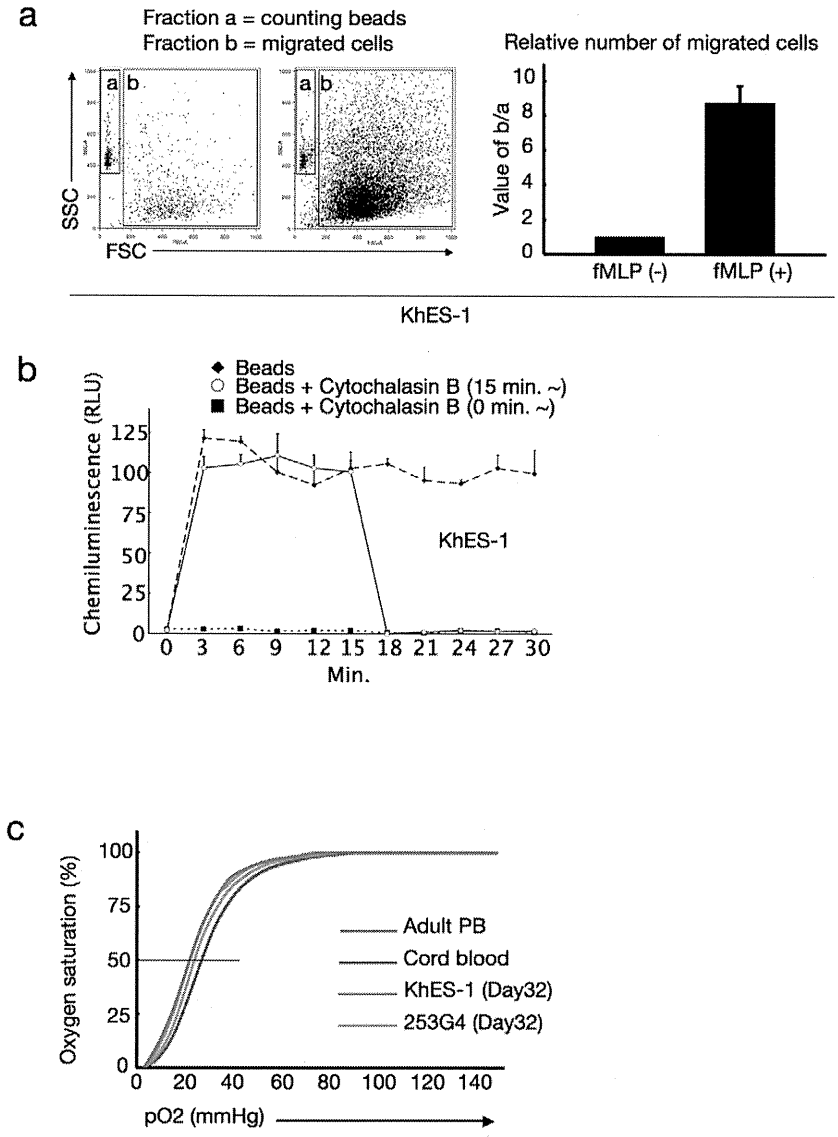

Figure 4. Functional blood cells derived from human ES/iPS cells. a. Number of migrated cells that permeated through the transwell membrane with or without fMLP. Values were normalised to the number of counting beads, and the control values were arbitrarily set to the condition without fMLP. Data from KhES-1 are shown as representative. **b.** Assay for phagocytosis-induced respiratory burst activity using chemiluminescent microspheres (luminol-binding microspheres). Abbreviation: RLU, relative light units. Data from KhES-1 are shown as representative. **c.** Oxygen dissociation curves of erythroid cells derived from human ES/iPS cells (harvested on day32 of differentiation), human cord blood, and adult peripheral blood. Where shown, bars represent standard deviation of the mean of three independent experiments.
doi:10.1371/journal.pone.0022261.g004

previous studies have demonstrated that ES cells can differentiate into the common multipotent progenitors that differentiate into both blood and endothelial cells at the single cell level on OP9 stroma [17,28,49]. Although the experiments described thus far demonstrated that the serum-free, xeno-cell-free culture condition supported human ES/iPS cell-derived hematopoiesis in an orderly manner, as observed during embryogenesis, it was unclear which day 6 fraction(s) developed into blood cells. To clarify this point, human ES cells stably expressing green fluorescent protein (GFP) were cultured, then 1×10^4 cells of $GFP^+KDR^-CD34^-CD45^-$ (Fraction A), $GFP^+KDR^+CD34^-CD45^-$ (Fraction B), and $GFP^+KDR^+CD34^+CD45^-$ (Fraction C) fractions were transferred on day 6 into a synchronous differentiation culture of unlabeled ES cells (Figure 6a). Nineteen days later (day 25 of differentiation), GFP^+ small round cell-containing colonies were observed predominantly in Fractions B and C, and FCM analysis of the entire culture confirmed the emergence of GFP^+CD45^+ cells mainly from Fraction C (Figure 6b). On the other hand, few blood cells positive for GFP were generated from Fraction A. These results were obtained with 2 independent strains of human ES cells (KhES1-EGFPneo on KhES-1 and KhES3-EGFPneo on KhES-3) (Figure 6c) and indicated that hematopoietic progenitors were present in the KDR^+ fraction, particularly in the KDR^+CD34^+ fraction, on day 6 of differentiation.

Finally, we performed a single-cell deposition assay by transferring single sorted human ES/iPS cell-derived $GFP^+KDR^+CD34^+CD45^-$ cells, which were negative for VE-cadherin, on day 6 into individual wells of 96-well plates coated

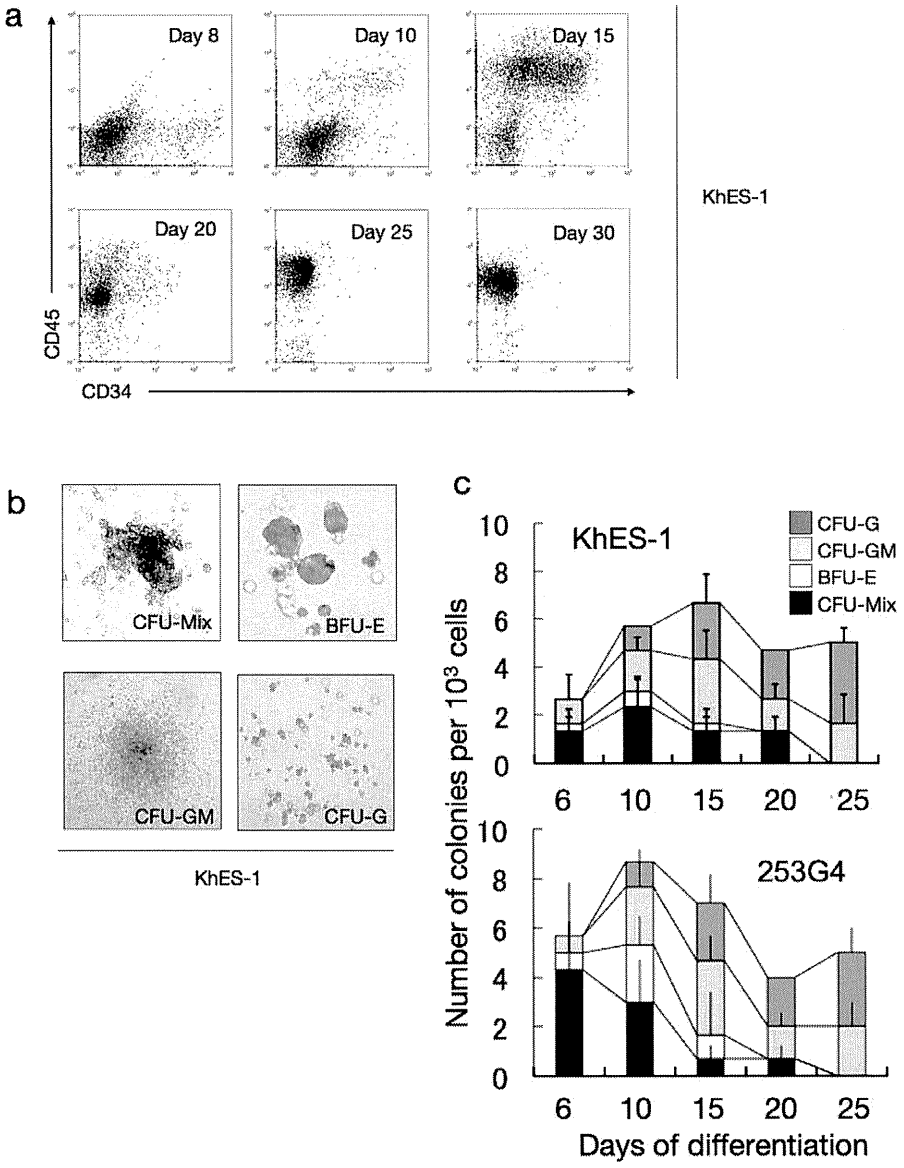

Figure 5. Hematopoietic stem/progenitor cells in culture. a. Sequential FCM analysis of cells harvested on indicated days showing the existence of $CD34^{+}CD45^{+}$ haematopoietic progenitor cells in culture. Data from KhES-1 are shown as representative. **b.** Various colony types on MTC-containing medium clonally emerged from single haematopoietic progenitor cells. Data from KhES-1 are shown as representative. **c.** Numbers of each colony type derived from different days of culture. Bars represent standard deviation of the mean of three independent experiments. Data from KhES-1 and 253G4 strains are shown as representative.
doi:10.1371/journal.pone.0022261.g005

with an OP9 cell layer. As shown in Figure 6d and e, the proportion of hematopoietic cell (HC) development, $VE\text{-}cadherin^{+}$ endothelial cell (EC) development, and HC plus EC development on day 20 were 9.0%, 6.8%, and 4.0%, respectively, for KhES-1 and 11.6%, 12.7%, and 8.3%, respectively, for 253G4 iPS cells. These results demonstrate that the common mesodermal progenitors that can differentiate into both blood and endothelial cells at the single-cell level are induced in our culture condition.

Discussion

In this study, we demonstrated the orderly mesodermal and hematopoietic differentiation of human ES and iPS cells in a novel serum-free monolayer culture condition. Simple manipulation of cytokine combinations facilitated robust, reproducible, and highly directed stepwise commitment to specific lineages of functional blood cells.

There are several reports on hematopoietic differentiation of human ES/iPS cells, such as murine-derived OP9 stromal cell coculture and feeder/serum-free EB formation systems [20,22,23,24,30,31,32,50]. However, two-dimensional cultures containing xeno-serum/cells often cause dependency on their lots, while complicated three-dimensional structures inside EBs make it difficult to assess and control conditions for inducing specific progenitors. Actually, few in vitro systems have been able to reliably reproduce hematopoietic development from mesodermal progenitors or model the in vivo coexistence of developing hematopoietic cells and their autologous microenvironments in

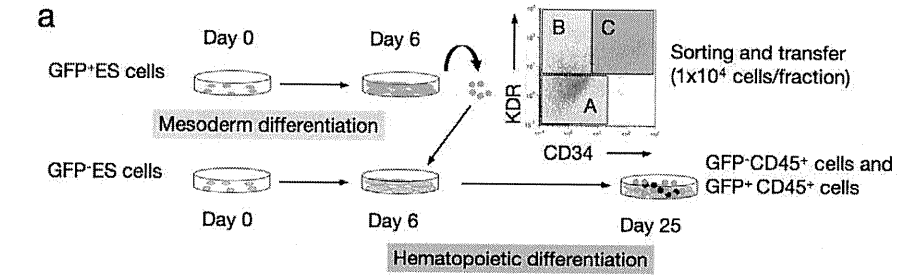

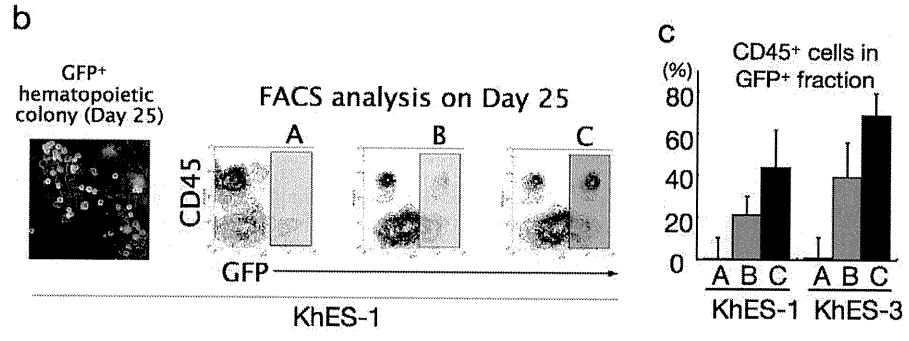

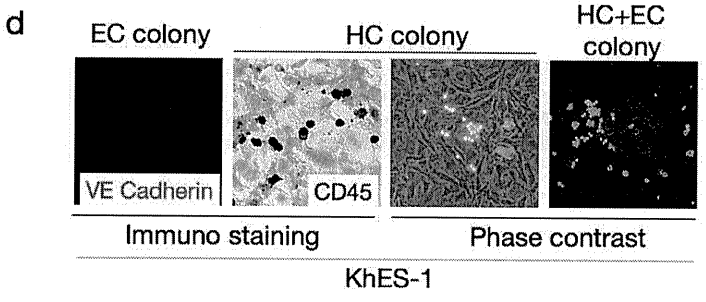

e

Clones	Only one cell 24 hours after sorting	At day 20		
		HC	EC	HC+EC
KhES-1 cells	176 wells	16 wells (9.0%)	12 wells (6.8%)	7 wells (4.0%)
256G4 iPS cells	181 wells	21 wells (11.6%)	23 wells (12.7%)	15 wells (8.3%)

HC : Haematopoietic colonies
EC : Endothelial colonies

Figure 6. Haematopoietic differentiation from KDR$^+$CD34$^+$ mesodermal progenitors. a. Schema of the protocol for measuring haematopoietic activities of depicted fractions on day 6. **b.** Each sorted fraction-derived haematopoiesis on day 25 detected by fluorescent microscopy and FCM analysis. Data from KhES-1 are shown as representative. **c.** Ratio of CD45$^+$ cells in GFP$^+$ fraction on day 25 showing the strongest haematopoietic activity of fraction C followed by fraction B. **d.** Single KDR$^+$CD34$^+$CD45$^-$ cell-derived haematopoietic colonies (HC), VE-cadherin$^+$ endothelial colonies (EC), and HC+EC colonies generated on OP9 cell layers. Data from KhES-1 are shown as representative. **e.** Number of wells that showed HC, EC, and EC+HC development.
doi:10.1371/journal.pone.0022261.g006

serum-free conditions. Our less labor-intensive and clearly defined monolayer culture facilitates observation of the stepwise development of pluripotent cells to blood cells via common hemoangiogenic progenitors and the behavior of hematopoietic cells on autologous stromal cells. Consequently, assays for elucidating differences in lineage specification of various ES/iPS cell strains, including hematopoietic potential, can be performed with high reproducibility. This is particularly important because individual pluripotent cell strains vary in differentiation potentials [51,52,53]. This study demonstrated quantitative differences in hematopoietic differentiation efficacy and lineage commitment among 4 ES/iPS cell strains.

Because human ES/iPS cells are feasible cell sources for various clinical applications, scientific and medical communities have shown continuing interest in hematopoietic stem cell induction from ES/iPS cells. Previous trials have indicated that murine ES cell-derived hematopoietic cells overexpressing HoxB4 [54] can replenish the bone marrow of lethally irradiated recipient mice. However, it remains a challenge to develop bona fide human hematopoietic stem cells with bone marrow reconstitution activity at the single-cell level. In our study, we observed many cobblestone area-forming cells, which reportedly indicate the existence of very immature hematopoietic progenitors. Moreover, FCM analyses and colony-forming assays suggested that ES and iPS human cell-